



Norwegian University
of Life Sciences

Master`s thesis 2023 60 ECTS

Faculty of Chemistry, Biotechnology and Food Sciences (KMB)

The impact of ADA2 downregulation on T-cell functioning of CRISPR/Cas9 edited PBMCs

Tuva Sundell

Biotechnology

The impact of ADA2 downregulation on T-cell functioning of CRISPR/Cas9 edited PBMCs



Norwegian University
of Life Sciences



Thesis submitted for the degree of Master of Science in Biotechnology
60 credits

Supervisors:

Dr. Emma Haapaniemi

Dr. Yasaman Pakdaman

Dr. Janna Saarela

Prof. Harald Carlsen

Center of Molecular Medicine Norway (NCMM)

and

The Norwegian University of Life Sciences

Faculty of Chemistry, Biotechnology and Food Sciences

May 2023

Acknowledgement

The work presented in this thesis was carried out in a collaborative project between Haapaniemi lab and Saarela lab at the Center for Molecular Medicine Norway (NCMM), Oslo from August 2022 to May 2023 under the supervision of Emma Haapaniemi, Yasaman Pakdaman, Janna Saarela and Harald Carlsen.

First, I want to thank both my main supervisor Emma Haapaniemi and Janna Saarela for having me as a student in their research groups. A special thanks goes to my daily supervisor Yasaman Pakdaman for devoting so much of her time supervising and helping me in the lab, and for her knowledge and insight into the laboratory work. I would also like to thank Harald Carlsen for being my internal supervisor at NMBU.

Additionally, I want to thank all members of the Haapaniemi and Saarela group for creating such a good workspace. You were very welcoming and helpful. It has been a privilege to be working with you all.

Finally, I want to thank my partner, friends, and family for all the motivation and support throughout this year.

Tuva Sundell

Ås, May 2023

Sammendrag

Deficiency of adenosine deaminase 2 (*ADA2* mangel, DADA2) er et uvanlig autosomt genetisk syndrom som er karakterisert ved autoinflammatoriske symptomer, hvor utviklingen av T-celler og B-celler ikke fungerer. DADA2 er forårsaket av mutasjoner som gir tap av funksjon i *CECR1* gen, som koder for enzymet adenosine deaminase 2. Adenosine Deaminase 2 (*ADA2*) er involvert i metabolismen av adenosine og har en rolle i reguleringen av immunrepsen, og enzymet har blitt koblet til reguleringen av T-celle aktivering og differensiering. Nylig forskning har foreslått at *ADA2*-nedregulering kan føre til endret T-celleaktivering og celle proliferasjon. Patogenesen til sykdommen er fortsatt ikke helt forstått.

Målet i dette studiet var å studere effekten av genaktiviteten og genuttrykket av å sette *ADA2* gen ut av funksjon, en så kalt «knock-out», og «knock-in» av *ADA2* mutasjonen R169Q. For så å studere hvordan nedreguleringen av *ADA2* påvirker T-celle funksjoner. Genredigeringen av T-celler ble gjort for å forstå mer av mekanismen av DADA2. Elektroporeringen ble brukt som en metode for CRISPR/Cas9 i PBMCs (perifere mononukleære blodceller) for «knock-out» av *ADA2* og «knock-in» av *ADA2* mutasjonen (R169Q), en mutasjon knyttet til utviklingen av DADA2. Videre ble cellene analysert for å evaluere *ADA2* enzymaktivitet og genuttrykk, og effekten av *ADA2* «knock-out» og R169Q mutasjonen på T-celler ble videre studert ved å bruke flow cytometri i T-celle aktivering og proliferasjons analyser.

En reduksjon i *ADA2* aktivitet og genuttrykk ble observert for både *ADA2* «knock-out» og «knock-in» av R169Q prøvene sammenlignet med ikke-redigerte celler. Derimot, for studiet av T-celle funksjon, oppsto det problemer ved lang dyrkning av de genredigerte T-cellene, som videre ble diskutert og sammenlignet med celler som hadde vært gjennom en kortere dyrkningsperiode.

Dermed er det nødvendig med fremtidige eksperimenter med et bredere sett av prøver fra flere donorer med forbedret redigeringseffektivitet. Det er avgjørende å optimalisere de eksperimentelle prosedyrene for bruk på redigerte celler for å få dypere innsikt i effekten av *ADA2*-nedregulering på T-cellefunksjonalitet. Å ta disse faktorene i betraktning, vil bidra til en mer omfattende forståelse av virkningen av *ADA2*-nedregulering på funksjonen til T-celler.

Abstract

Adenosine Deaminase 2 Deficiency (DADA2) is a rare autosomal genetic syndrome characterized by auto-inflammatory symptoms, where the development of T lymphocytes and B lymphocytes is malfunctioning. The deficiency is caused by the loss of function mutations in the *CECR1* gene, which encodes the enzyme adenosine deaminase 2. Adenosine Deaminase 2 (ADA2) is involved in the metabolism of adenosine and has a role in regulating the immune response, and in addition it has been linked to the regulation of T-cell activation and differentiation. Recent studies suggest that downregulation of ADA2 can lead to altered T-cell activation and proliferation. The pathogenesis of the disease is still not completely understood.

The aim of this study was to study the effect of knock out of *ADA2* and knock in of *ADA2* R169Q mutation on the activity and expression of the *ADA2* gene. and study the impact of ADA2 downregulation on T-cells functioning. The editing on T-cells was done to understand more of the mechanism of DADA2. Electroporation was used as delivery method for CRISPR/Cas9 in PBMCs (Peripheral Blood Mononuclear Cells) to knock out the *ADA2* gene and knock in a mutation of ADA2 (R169Q), a mutation linked to the development of ADA2 deficiency. Further the cells were analyzed to evaluate ADA2 enzyme activity and gene expression, and the effect of ADA2 knockout and R169Q mutation on T-cells were studied using flow cytometry in T-cell activation and proliferation downstream assays.

A decrease in ADA2 activity and gene expression were observed for the ADA2 KO and KI of R169Q samples compared to the non-edited samples. However, for the study of T-cell functioning, some problems occurred for long cultivation of the edited T-cells, which was further discussed and compared with cells undergoing a shorter cultivation period.

Thus, future experiments are needed with a wider set of samples from multiple donors with enhanced editing efficiency. It is crucial to optimize the experimental procedures for utilizing edited cells to gain deeper insights into the effects of ADA2 downregulation on T-cell functionality. Taking these factors into consideration will contribute to a more comprehensive understanding of the impact of ADA2 downregulation on the functioning of T-cells.

Abbreviations

ADA	Adenosine deaminase
CFSE	Carboxyfluorescein succinimidyl ester
CRISPR	Clustered regulatory interspaced short palindromic repeats
DADA2	Deficiency of adenosine deaminase 2
dATP	Deoxyadenosine triphosphate
ddH₂O	Double distilled water
ddPCR	Digital droplet polymerase chain reaction
DMSO	Dimethyl Sulfoxide
DNA	Deoxyribonucleic acid
DNase	Deoxyribonuclease
FMO	Fluorescence minus one
FSC	Forward scatter
FSC-A	Forward scatter area
FSC-H	Forward scatter height
SSC	Side scatter
gRNA	Guide RNA
HDR	Homology-directed DNA repair
IL-2	Interleukin-2
IL-7	Interleukin-7
IL-15	Interleukin-15
KI	Knock in
KO	Knock out
NFW	Nuclease-Free Water
NHEJ	Non-homologous end-joining
PBMC	Peripheral blood mononuclear cell
PHA	Phytohemagglutinin
RNA	Ribonucleic acid
RNP	Ribonucleoprotein
TCR	T-cell receptor
WT	Wild type

1 Table of Contents

Acknowledgement	II
Sammendrag.....	III
Abstract	IV
Abbreviations	V
1 Introduction.....	1
1.1 The Immune System.....	1
1.1.1 Hematopoiesis.....	1
1.1.2 Innate immunity	2
1.1.3 Adaptive immunity	3
1.2 T-cell Biology.....	4
1.2.1 Structure and function of T-cells	4
1.2.2 T-cell subsets	4
1.2.3 T-cell activation and proliferation	6
1.3 Primary Immunodeficiency Diseases	7
1.4 ADA2 Deficiency.....	7
1.4.1 Clinical picture of DADA2	7
1.4.2 Molecular pathogenesis of ADA2 enzyme	9
1.4.3 ADA1.....	9
1.4.4 The role of ADA2 enzyme in cell biology	10
1.4.5 R169Q mutation	10
1.5 Genome Editing.....	10
1.5.1 CRISPR/Cas9	10
1.5.2 CRISPR/Cas9 using electroporation.....	13
1.6 Isolation of T-cells.....	13
1.7 Digital Droplet PCR	14
1.8 Flow Cytometry.....	15
1.9 Aims of the Thesis.....	15
2 Materials and methods	17
2.1 Materials.....	17
2.2 Designing PCR Primers.....	17
2.3 PBMC work: <i>ADA2</i> Gene Editing of Human PBMCs	20
2.3.1 Cultivation of Peripheral Blood Mononuclear Cells (PBMCs).....	20
2.3.2 Electroporation.....	21
2.4 DNA Isolation	22

2.5	Qubit.....	22
2.6	Digital Droplet PCR (ddPCR).....	23
2.6.1	Statistical Analysis	24
2.7	<i>ADA2</i> Activity Test in CRISPR/Cas9 <i>ADA2</i> Knock Out and WT PBMCs using Diazyme Kit 25	
2.7.1	Lysis of the cell	25
2.7.2	BCA assay.....	25
2.7.3	Activity test in PBMC using Diazyme kit.	25
2.8	Evaluation of Downregulated <i>ADA2</i> Transcription.....	27
2.8.1	RNA isolation	27
2.8.2	cDNA synthesis	27
2.8.3	Real-time quantitative RT-PCR	28
2.9	Flow Cytometry and Fluorescent Staining of T-cells.....	29
2.9.1	Pre-stimulation for activation and proliferation assays	29
2.9.2	Stimulation of T-cells for activation and proliferation assays	30
2.9.3	Antibody staining.....	31
2.9.4	Flow cytometry.....	32
3	Results.....	34
3.1	<i>ADA2</i> Editing in T-cells	34
3.2	Evaluation of <i>ADA2</i> Gene Knockout and Knock Kn of R169Q Mutation.....	38
3.3	Evaluation of The Loss of <i>ADA2</i> Transcript in <i>ADA2</i> Knockout and Knock In of R169Q Mutation	39
3.4	Effect of <i>ADA2</i> Knockout and R169Q Mutation Knock in on T-cells.....	40
3.5	The Effect of Long Culturing vs Short Culturing on CRISPR/Cas9 Edited PBMCs for T-cell Activation Assay	42
3.6	Effect of Long Culturing vs Short Culturing on CRISPR/Cas9 Edited PBMCs for T-cell Proliferation Assays using CFSE Staining	47
4	Discussion	50
4.1	<i>ADA2</i> Editing in T-cells	50
4.2	Downregulation of <i>ADA2</i> Gene Expression Gave Lower Protein Activity	51
4.3	Variability in T-Cell Activation and Proliferation Assays with Long-Cultured Edited T- Cells"	54
4.4	Concluding remarks and future perspectives.....	57
5	Appendix I	58
6	Appendix II.....	62
7	References.....	69

1 Introduction

1.1 The Immune System

1.1.1 Hematopoiesis

Hematopoiesis is defined as the production of all blood cell components, from the hematopoietic stem cells (HSCs). This cell production occurs within the hematopoietic system, containing organs and tissues such as bone marrow, thymus, spleen, and lymph nodes. Production and renewal of the blood cells begin in embryonic development and continue throughout adulthood (Jagannathan-Bogdan & Zon, 2013). HSCs have the ability to differentiate into all mature blood lineages, which include erythrocytes, lymphocytes, platelets, granulocytes, and monocytes (Hoggatt & Pelus, 2013).

Each of these different blood cell types is produced through different pathways in the hematopoietic system. Within the HSCs, the process divides into two pathways; the first pathway is the lymphoid pathway, being in charge of producing key components of adaptive immunity, lymphocytes, which then again will differentiate into T-cells, B-cells and natural killer cells (NK cells). The second pathway is the myeloid pathway, being responsible for producing innate immune cells including monocytes, granulocytes, erythrocytes and platelets (Kondo, 2010).

Differentiation of Hematopoietic Stem Cells

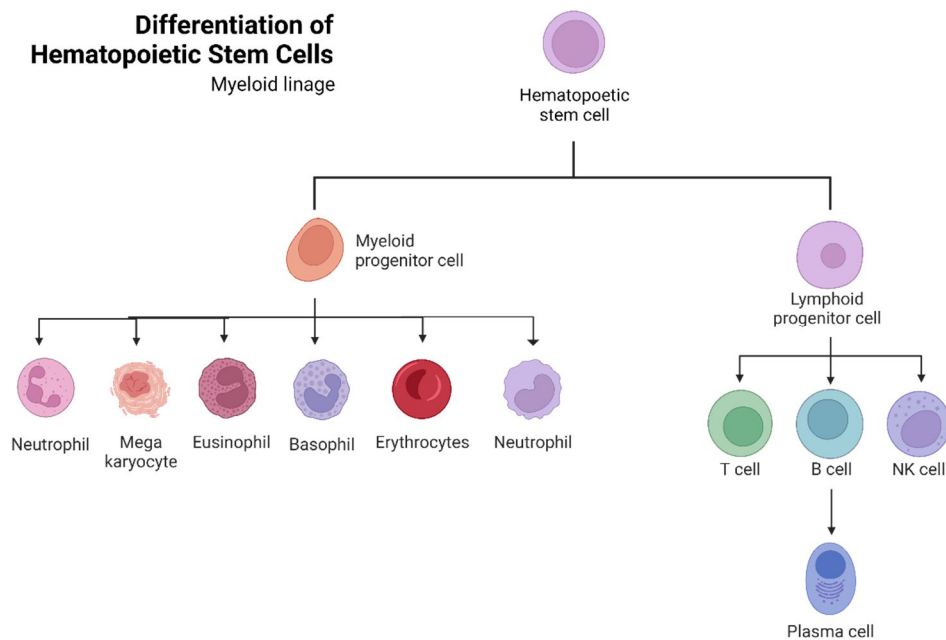


Figure 1.1 Differentiation of Hematopoietic Stem cells.

The figure presents a schematic representation of the hematopoietic hierarchy, illustrating the hierarchical organization of different cell types involved in the process of hematopoiesis, the formation of blood cells. Hematopoiesis is the intricate process by which HSCs give rise to different types of blood cells, including red blood cells, white blood cells, and platelets. A hematopoietic stem cell can differentiate into either myeloid progenitor cell or a lymphoid progenitor cell. Common lymphoid progenitor cells can then again differentiate into natural killer cells (NK cells), T-cells, or B-cells (on right). While the myeloid progenitor cells can differentiate into neutrophils, megakaryocytes, eosinophils, basophils, erythrocytes, or neutrophils. Figure is made by author using Biorender with inspiration from (Raza et al., 2021).

1.1.2 Innate immunity

The immune system can be separated into two systems: innate and adaptive immunity. The innate immunity generate a non-specific response against the pathogen while adaptive generate a specific immune response against a particular type of pathogen (Parham, 2021, pp. 10-14).

Innate immunity is the first line of defense against any intruder. Its primary goal is to prevent any intruder from entering the body and will therefore protect the body against all antigens. Innate immunity involves barriers that keep these harmful intruders from entering the body. These barriers include physical barriers like skin and mucus, and chemical barriers as for example enzymes in tears and skin oils, and stomach acid (Aristizábal & González, 2013). The next line of defense in the innate system is inflammation, which is performed by the mast cells. The mast cells are constantly searching for suspicious objects in the body. When the mast cells find an external antigen, they release histamine molecules, which alert the body as a signal and increase blood flow to that specific area, resulting in inflammation (Theoharides et al., 2012). Leukocytes, which are transferred through the blood, consists of different cell types, and the

ones that are involved in the innate system are the phagocytes, including macrophages, neutrophils, and dendritic cells (Parham, 2021, pp. 17-18). Phagocytes such as neutrophils patrol the body by killing the infected cells and then dying. The macrophages engulf pathogens and instead of roaming around freely, they get collected at certain places in the body (Parham, 2021, p. 18).

Another type of cell involved in the innate system is also the natural killer (NK) cell which can detect infected cells. The NK cells detect a protein on the normal cell surface called the Major Histocompatibility Complex (MHC) which is absent in abnormal cells (Vivier et al., 2011). Dendritic cells are the last line of defense within the innate system. They are found in the parts of the body that are connected to the external environment, like the lungs and nose. Dendritic cells are the links between the innate and adaptive system. These dendritic cells consume pathogens and send information about them to the T-cells of the adaptive system in the form of an antigen (Banchereau et al., 2000).

1.1.3 Adaptive immunity

The adaptive system is the second line of defense and can differentiate between different types of pathogens. This system contains the T- and B lymphocytes (Iwasaki & Medzhitov, 2010). The T-cells-related immunity comes into action when the infection has already occurred and is called the cell-mediated immune response. B-cells, however, act on the pathogens that have entered the body but have not caused any disease yet in a process called the humoral immune response. Those T-cells that take signals from the dendritic cells or macrophages are named helper T-cells and have CD4 molecules as a surface marker. The helper T-cells have two tasks: forming effector T-cells and memory T-cells. Cytotoxic T-cells are another type of T-cell that have CD8 molecules on their cell surfaces and can regulate the infection by killing infected cells directly (Stockwin et al., 2000). B-cells produce antibodies that detect the antigen of the pathogens. The antibodies act as signals to the macrophages for killing the pathogens. B-cells produce memory B-cells when they encounter an antigen. Memory B- and T-cells maintain a record of encountered infections and therefore strengthen the immune system's response to the reoccurrence of these infections (Parham, 2021, p. 308).

1.2 T-cell Biology

1.2.1 Structure and function of T-cells

T-cells are a type of leukocyte and are designed to fight infections they have not encountered yet. These cells mature in the thymus and when needed, they get released into the bloodstream as naïve T-cells, where they search for an antigen-presenting cell (APC) (Akadeum Life Sciences, 2020).

T-cells have a central role in the arrangement of all the functions of adaptive immunity, where the four most important tasks include inflammation by cytokine production, elimination of unwanted cells, assisting B-cells and regulation of immunosuppressive responses (B. Alberts et al., 2002a).

T-cells originate from the hematopoietic stem cells of the bone marrow and use somatic recombination and mutation to produce functional genes that encode the T-cell antigen receptors (TCR).

The T-cell receptor (TCR) is a molecule that is found on the surface of the T-cells and is in charge of recognizing fragments of antigen when foreign peptides, derived from pathogens or tumors, bind to the MHC. There are two different types of TCR based on two different protein chains, the $\alpha\beta$, containing alpha-beta chains, which are the ones responding to MHC with antigen, and the $\gamma\delta$, containing gamma-delta chains (B. Alberts et al., 2002b).

1.2.2 T-cell subsets

Leukocytes exhibit a diverse array of molecules on their cell surfaces that reflect various stages of their lineage-specific differentiation or activation and inactivation states. Cluster of differentiation (CD) is a surface marker that identifies a particular differentiation lineage recognized by a group of monoclonal antibodies. This classification of the antigens is called clusters of differentiation (CDs) ("3 - CLUSTER OF DIFFERENTIATION (CD) ANTIGENS," 2004).

T-cells are divided into two major groups: CD4- and CD8- cells, and are identified by CD3+, which is a protein complex and T-cell co-receptor (Rishi Vishal Luckheeram et al., 2012).

The CD8⁺ T-cells kill targeted cells, and this group is categorized into at least two subgroups expressing different chemokine receptors: Tc1 and Tc2. CD8⁺ T-cell subpopulations are specialized to combat intracellular pathogens (Delfs et al., 2001).

The CD4⁺ T-cells function as helpers on other cells. Their activation leads to the secretion of cytokines that help regulate other types of cells. CD4⁺ are again divided based on the type of secreted cytokines into the subsets Th1, Th2, Th9, Th17 and T-reg groups. CD4⁺ T-cell subpopulations are specialized to combat extracellular pathogens (Rishi Vishal Luckheeram et al., 2012).

CD4⁺ T-cell developed from the $\alpha\beta$ T-cell can activate macrophages (R. V. Luckheeram et al., 2012). The CD4s can also interact with B-cells, which will lead to the B-cell responses with production of antibodies from plasma cells. (Zhu & Paul, 2008).

The first a T-cell does is to develop into a $\gamma\delta$, or an $\alpha\beta$ T-cell. T-cells presenting the $\alpha\beta$ or $\gamma\delta$ chains later develop into either a CD8⁺ T-cell or a CD4⁺ subtype. T-cells that react to the body's own antigens will be removed (Parham, 2021, pp. 132-133). There is a lack of information regarding $\gamma\delta$ T-cells, but it is known that they are not capable of recognizing MCH and that they secrete cytokines, including interleukin (IL)-4, IL-10, and IL-17, and the inflammatory cytokines interferon- γ (IFN- γ) and tumor necrosis factor (TNF)- α (Ramstead & Jutila, 2012).

Positive selection ensures that the T-cells can recognize MHC molecules. If a T-cell recognizes a MCH class I, it will downregulate the CD4⁺ transcription and will only have CD8⁺ in its membrane and is now single positive for CD8⁺. While the T-cells that recognize the MCH class II will do the same, but with CD4 (B. Alberts et al., 2002b).

After the positive selection the T-cell can bind MHC, but it is a risk, as it might bind MHC with self-peptide if it is released into the circulation. The risk is to become autoreactive T-cells that may turn out to be harmful and cause autoimmunity. The next step is therefore to remove those T-cells that recognize the body's own antigens, called negative selection (Starr et al., 2003).

An important early marker of T-cell activation is CD69 (Cibrián & Sánchez-Madrid, 2017). In a normal immune response CD69 is a cell surface glycoprotein expressed in cell activation and is important for the survival of activated T-cells and proliferation of the cells.

Expression of CD69 happens through Interleukin-2 (IL-2) receptor or T-cell receptor (TCR). IL-2 receptors are composed of an alfa chain (α), beta chain (β) and a gamma chain (γ). The

CD25 is the alpha chain of IL-2, and this α -chain is regarded to be the cellular activation marker of the greatest significance. (Bajnok et al., 2017). The very early activation marker CD69 is detectable within hours of cell activation, however, is lost after 48-72 hours (Borges et al., 2007).

1.2.3 T-cell activation and proliferation

For an immune response to be effective, and for the immune system to be able to both recognize and remove specific antigens, while also establishing a long-term immune memory, T-cell activation and proliferation are crucial (Janeway & Bottomly, 1994).

The first step of T-cell activation is recognition of the specific antigens, which are small foreign protein fragments from either pathogens or abnormal cells (B. Alberts et al., 2002b). The antigens are presented to T-cells by antigen-presenting cells (APCs), such as the dendritic cells and macrophages. By the use of the MHC protein, The APCs presents the antigen on the surface of the cells. The TCR will bind to the antigen-MHC complex as described in section 1.2.1. Additionally, co-stimulatory signals are for a complete T-cell activation to occur. Co-stimulatory molecules, including CD28 on T-cells, provides a second signal that contributes to avoid unnecessary activation from happening and ensures that the T-cell response is suitable (Esensten et al., 2016).

The TCR binding and the co-stimulatory signals will trigger intracellular signals in the T-cell, leading to activation of the T-cell (Shah et al., 2021).

CD3 is a protein complex involved with the TCR to create an activation signal in both the cytotoxic T-cells (CD8+) and helper T-cells (CD4+) (Yang et al., 2005). Phytohemagglutinin (PHA) is a mitogen derived from plants, which is used in laboratories for stimulation of T-cell proliferation. PHA activates T-cells by directly stimulating the TCR complex, skipping the antigen recognition step, and result in production of cytokines and T-cell proliferation (Kay, 1991).

Once the cell is activated, the cell will undergo clonal expansion, which is a proliferation step resulting in the T-cell population specific to the encountered antigen expanding (Stockwin et al., 2000). During this step, the T-cells differentiates into the different subsets with specific functions, described in section 1.2.2.

The now expanded and differentiated T-cells known as effector T-cells, have specific purposes for eliminating the antigen (Janeway CA Jr et al., 2001). The CD8⁺ cells will directly kill targeted cells, while the helper T-cells secrete cytokines that help regulate other types of cells as described in section 1.2.2.

1.3 Primary Immunodeficiency Diseases

Malfunctioning of immune cells can lead to diseases known as immunodeficiencies. These disorders will hinder the immune system's ability to defend the body against foreign or untypical cells including cancer cells, bacteria, viruses, and fungi, making the individual less prone to infection and diseases, such as autoimmunity disorders, cancer, and allergies (Dropulic & Lederman, 2016).

There are two main categories of immunodeficiencies: primary immunodeficiency, which is present from birth, and secondary immunodeficiency, which develops later in life (Sánchez-Ramón et al., 2019).

Abnormalities in genes that affect the development or proper functioning of immune cells typically cause primary immunodeficiencies, which often become apparent during infancy or early childhood. Primary immunodeficiency (PID) is a heterogenous group of disorders, and patients with PID are more likely to suffer severely from infections. Over 250 types of PID have been genetically identified, with new disorders constantly being identified (Al-Herz et al., 2014).

1.4 ADA2 Deficiency

1.4.1 Clinical picture of DADA2

Deficiency of ADA2 (DADA2) is a rare autosomal recessive auto inflammatory syndrome, where the development of T lymphocytes and B lymphocytes is malfunctioning. It's caused by the loss of function mutations in the *CECRI* gene that encodes the enzyme adenosine deaminase enzyme 2 (ADA2) (Vogan, 2014). Most of the mutations are missense, however there have been reported genomic deletions, nonsense, and splicing mutations. Mutations associated with DADA2 are either unreported or found at a low allele frequency (< 0.001) in public databases (Isabelle Meyts & Ivona Aksentijevich, 2018). These mutations result in

reduced or absent plasma ADA2 enzymatic activity. Over 60 disease-associated mutations are identified in the domains of ADA2, and affect protein dimerization, secretion, and the catalytic activity (I. Meyts & I. Aksentijevich, 2018).

The most common disease mutation variants are Gly47Ala, Gly47Arg, Arg169Gln, and Tyr453Cys, which are most frequently found in founder populations. For instance, Arg169Gln, known as R169Q, is known as a founder mutation in Belgian, Dutch, and Finnish populations, having a carrier frequency of 1:500 in Northern European populations (Meyts, Isabelle & Aksentijevich, Ivona, 2018).

ADA2 deficiency in clinical cases exhibits significant variability among patients. At present over 170 patients have been reported with around 25% of patients experiencing symptoms before reaching age 1, while the majority of cases arise prior to the age of 10 years (Moens et al., 2019).

Clinical features of DADA2 includes vasculitis and inflammation that can act on several organs, which explains the manifestations being hepatological, intestinal and renal (I. Meyts & I. Aksentijevich, 2018).

ADA2 deficiency is associated with considerable mortality rates, as up to 8% of patients may not survive past the age of 30 years due to the condition (Moens et al., 2019).

Hematological phenotypes exist in some patients. Hematological symptoms primarily involve hypogammaglobulinemia, which is the most prevalent manifestation in ADA2 deficiency cases. However, there has been a growing number of reported cases indicating additional hematological complications such as pure red cell aplasia (PRCA), immune thrombocytopenia, and neutropenia (Isabelle Meyts & Ivona Aksentijevich, 2018). PRCA, a rare disorder characterized by a decrease in red blood cell production in the bone marrow, have been confirmed in 3 patients (Ben-Ami et al., 2016; Hashem et al., 2017).

In the matter of treatment of DADA2, current therapies include hematopoietic stem cell transplantation to replace the stem cells that will mature into the B- and T lymphocytes and have been showing success in some patients (Aksentijevich I et al., 2019). Another treatment is enzyme replacement therapy with intramuscular injections of the active ADA enzyme. However, for stem cell transplantation, patients often suffer from a variety of physiological problems, and for the enzyme therapy, complications arise and the effectiveness of the treatment declines after 8-10 years (Cox & Nelson, 2021, p. 900).

1.4.2 Molecular pathogenesis of ADA2 enzyme

The ADA2 protein is immensely expressed in myeloid cells and has a role in the differentiation of macrophages, however the function of the protein is still much unknown (Andrey V Zavialov et al., 2010).

ADA2 catalyzes the deamination of adenosine and 2'-deoxyadenosine to inosine and deoxyinosine. ADA2 is a secreted protein that is hypothesized to regulate a variety of biological processes and control the amount of extracellular adenosine. The regulation happens through 4 adenosine receptors which are expressed on cells both in the immune and cardiovascular systems, and the brain (Zavialov & Engström, 2005).

ADA2 has been identified to act as a growth factor, belonging to a group of ADGFs (ADA-related growth factors), found in almost all organisms. The function of the ADGFS is still much unknown, however their growth factor activity is linked with ADA2 activity (Dolezal et al., 2005).

The ADA2 dimeric protein is secreted into the extracellular space, where it has anti-inflammatory action and functions as a deaminase to control adenosine levels at the site of inflammation. Consistently, ADA2 levels are elevated in plasma samples of patients with infectious diseases or chronic inflammation. Disease-associated mutations affect the catalytic activity, protein dimerization, and secretion of ADA2. (Vinchi, 2021).

1.4.3 ADA1

The ADA enzyme is represented by two isoenzymes: ADA1 and ADA2. The ADA1 isoenzymes are found in all cells, with the highest activity in lymphocytes, whereas ADA2 isoenzymes appear to be found only in antigen-presenting cells.

ADA is represented by the two isoenzymes ADA1 and ADA2. The already described ADA2 are found only in cells presenting antigen, while ADA1 isoenzymes are found in all type of cells, where the highest ADA1 activity is found to be in lymphocytes (Kaljas et al., 2017).

The result of the ADA1 dysfunction is increased accumulation of deoxyadenosine triphosphate that interfere with normal DNA replication, and collapses the lymphocyte immune system by disabling proliferation, which leads to severe combined immune deficiency (ADA-SCID) (Flinn & Gennery, 2018).

1.4.4 The role of ADA2 enzyme in cell biology

The deoxyadenosine triphosphate (dATP) nucleotides are needed in equal proportions to make cellular division go smoothly. These nucleotides have a functional lifespan, and will then be broken up, and either recycled or secreted. The task of the adenosine deaminase enzyme is to remove an amine group from dATP, in the process of making uric acid of dATP, for secretion. Lymphocytes are cells that divide rapidly and therefore rely heavily on cell division (Flinn & Gennery, 2018).

In ADA2 syndrome, dATP will no longer be degraded because it is not needed, and will pile up, and will slow down the process of cell division that further will affect cells throughout the body, especially the lymphocytes. The number of lymphocytes will go down, and collapse the immune system (Flinn & Gennery, 2018).

1.4.5 R169Q mutation

R169Q is an *ADA2* disease relevant mutation locus C→T (R169Q), with high frequency in Finnish and Northern European populations (Jee et al., 2022). It is an autosomal recessive mutation with clinical phenotypes including Aplastic anemia, large granular lymphocyte leukemia and vasculitis. Research has shown that patients with R169Q mutation, have a lower adenosine deaminase 2 enzyme activity (Van Montfrans et al., 2016).

1.5 Genome Editing

Genome editing is a group of genetic engineering technologies in which DNA can be inserted, removed, replaced, or adjusted in the genome of a living organism (Doudna, 2020). A well-known method of genome editing called CRISPR-Cas9, is cheaper, more accurate and more efficient than other genome editing technologies (Adli, 2018).

1.5.1 CRISPR/Cas9

Since the year 2012, the use of the gene-editing tool CRISPR/Cas9, short for Clustered Regularly Interspaced Short Palindromic Repeats, has allowed scientists to introduce specific mutations at a targeted site in the genome of animals, plants, microorganisms, and fungi. This technique is known to be more precise and efficient compared to other targeting methods, such

as Zinc-finger nucleases (ZFNs) and Transcription activator-like effector nucleases (TALENs) (Adli, 2018).

For the CRISPR/Cas9 method, an enzyme called Cas9 is needed, which acts like a pair of scissors by cutting the two DNA strands at specific locations in the genome, allowing bits of DNA to be added or removed to the sequence (Adli, 2018).

By using CRISPR/Cas9 technique, one would also typically need a single-guide RNA (sgRNA) that can easily be altered to target specific sites in the genome. gRNA is composed of the two elements: Crispr RNA (crRNA) and Trans-activating crRNA (tracrRNA) (Jinek et al., 2012). CrRNA is complementary to the target DNA strand and will therefore match with the sequence. TracrRNA is the second part of the gRNA and serves as a scaffold for the Cas9 protein, and therefore guides the Cas9 towards the targeted DNA (Adli, 2018). For the Cas9 to make a double-stranded DNA break within the targeted sequence, a short motif called protospacer adjacent motif (PAM) needs to be placed 3-4 nucleotides downstream from the cut site (Doudna, 2020).

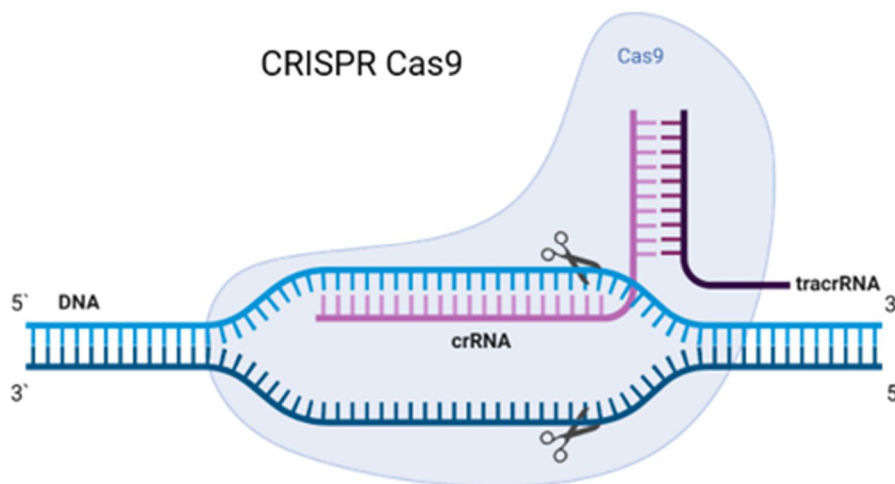


Figure 1.2: an overview of the CRISPR (Clustered Regularly Interspaced Short Palindromic Repeats) genome editing tool.

The figure showcases its key components and the steps involved in the editing process. The Cas9 binds to a targeted DNA sequence with the gRNA, that is made up of two parts: crispr RNA (crRNA) (purple) and trans-activating CRISPR RNA (tracrRNA) (black), which induces double strand breaks in the complementary strand (light blue) and in the non-complementary strands (dark blue). Cas9 then cuts the DNA at the target site, creating a double-stranded break. Figure created by author in biorender.

To induce a double-stranded break, the cells have evolved two DNA repair mechanisms. The non-homologous end joining (NHEJ) repair pathway is the most common pathway where the

cleaved ends of the DNA strand are directly joined together, as you can see in figure 1.3. NHEJ commonly induces insertions or deletions of nucleotides in the DNA sequence, known as indels (Chakrabarti et al., 2019). These indels often lead to silent frameshift changes in the DNA sequence or inducing nonsense mutations, that can be used for knocking out genes giving disease with the use of CRISPR/Cas9 (Zhang, 2021).

The second repair pathway is Homology-directed repair (HDR) (He et al., 2016). This mechanism is a more precise process where the DNA double-strand break in the sequence is repaired by homologous recombination using a donor template, as seen in figure 1.3 (Zhang, 2021). The use of the CRISPR-Cas9 gene-editing system's mechanism for introducing designed DNA templates in knock in experiments are therefore based on the HDR repair pathway.

The HDR repair pathway facilitates highly accurate gene editing via CRISPR-Cas9, which can be applied to clinical purposes. CRISPR/Cas9-based genome editing has become a promising tool in gene therapy for treating human genetic diseases, including cancers and cardiovascular diseases (Zhang, 2021).

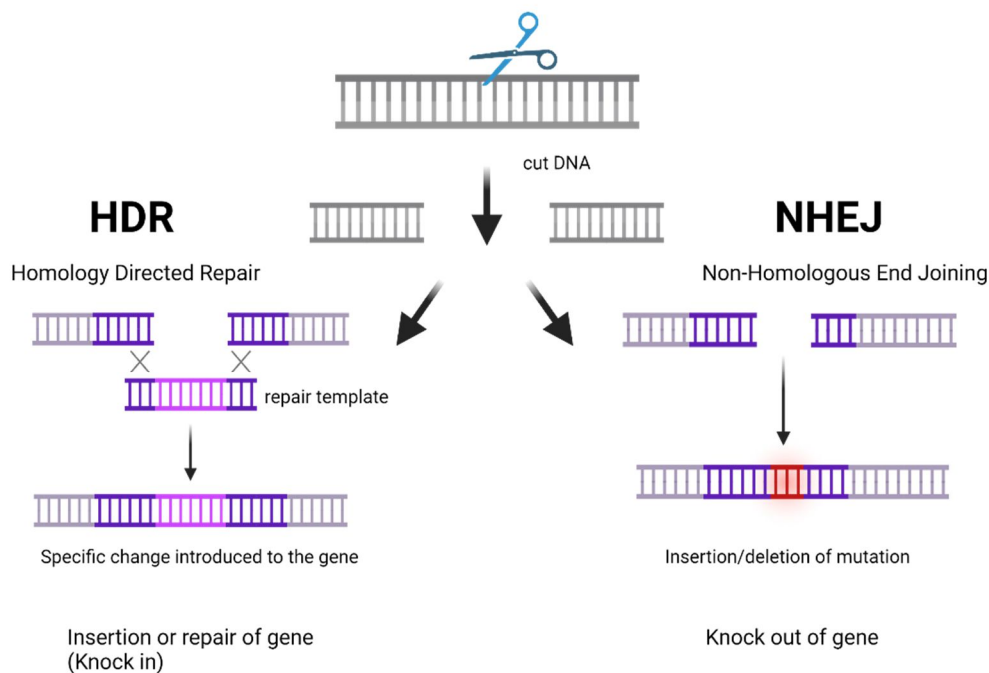


Figure 1.3: The figure illustrates two DNA repair pathways: Non-Homologous End Joining (NHEJ) and Homology-Directed Repair (HDR). These pathways play essential roles in the repair of DNA double-strand breaks (DSBs) and are commonly utilized in conjunction with the CRISPR genome editing tool. NHEJ (on the right) directly ligates broken DNA ends together without a template. This can result in the insertion or deletion of genetic material, leading to gene disruption or knockout. HDR (on the left) uses a template DNA sequence that is homologous to the broken DNA ends for precisely repairing

the double-strand breaks. By incorporating desired genetic modification from the template, HDR allows for targeted gene editing and precise genetic alterations. Figure made by author on Biorender.

1.5.2 CRISPR/Cas9 using electroporation

Electroporation is an effective tool to introduce foreign DNA together with CRISPR/Cas9 components into target cells. The method involves application of brief electrical pulses creating temporary pores in the cell membrane, which promote the delivery of exogenous molecules. By combining electroporation with CRISPR/Cas9, researchers can directly into the cells introduce the necessary components for genome editing, which again will allow for targeted modifications to the DNA sequence (Yarmush et al., 2014).

Electroporation is known to have high transfection efficiency and demonstrates a wide range of applicability, allowing for effective delivery of CRISPR/Cas9 components in diverse cell types, and offers a range of advantages compared to other transfections methods, like viral vectors and lipid-based transfection, that require usage of viral particles and carriers.

Electroporation therefore also minimize the immunogenicity concerns that are connected with the other transfection methods mentioned (Yarmush et al., 2014).

1.6 Isolation of T-cells

Isolating human T-cells is a process that normally starts with separating the buffy coat from whole blood from healthy blood donors or patients. After centrifugation of the whole blood, the buffy coat is the thin layer between the plasma and serum that contains most of the lymphocytes and thrombocytes (Sutton et al., 1988). The peripheral blood mononuclear cells (PBMCs) are then isolated from the buffy coat. The PBMCs are all the blood cells that has a round nucleus, and is therefore the part of the buffy coat containing the monocytes, lymphocytes, natural killer cells and dendritic cells (Kleiveland, 2015). The obtained PBMCs are then cultured in T-cell expansion medium, which includes the cytokines IL-2, 7 and 15. These cytokines will select and activate the T-cells from the PBMCs.

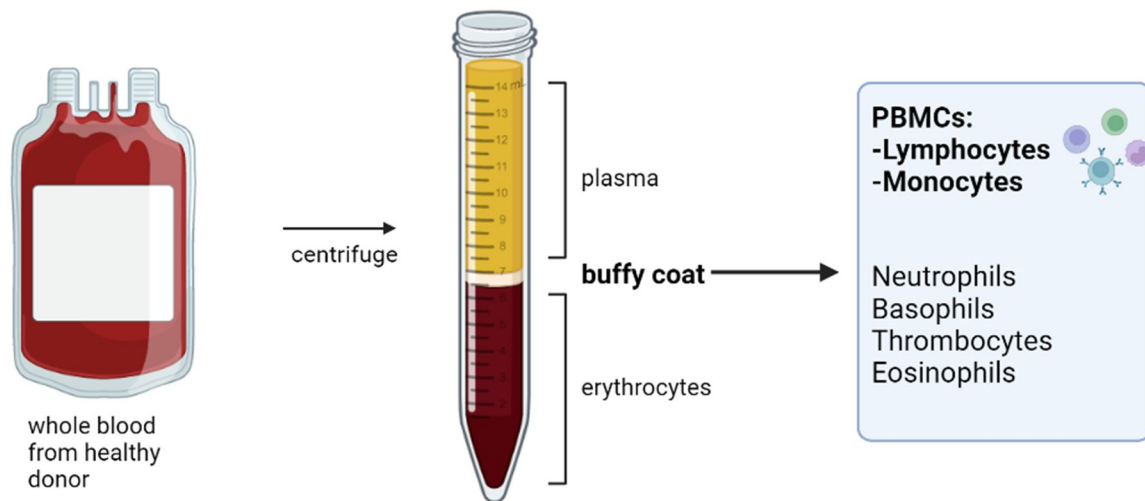


Figure 1.4: the process from whole blood to PBMCs.

After centrifugation, the whole blood will separate into two layers where the top layer is plasma, and bottom layer the erythrocytes. Between the layers, is the buffy coat that contains consists of the leucocytes. This figure was made with BioRender by the author.

1.7 Digital Droplet PCR

Digital Droplet PCR (ddPCR) is a method for performing quantitative DNA measurements. Like real-time PCR, ddPCR uses a simple sample preparation that utilizes TaqMan primers and probes, and an optimized supermix. ddPCR provides an absolute quantification of the sequences of the targeted DNA compared to real-time PCR that gives relative quantification (Bio-Rad). The measurements count absolute quantities of nucleic acid molecules that are encapsulated in water-in-oil droplet partitions, where PCR is performed on each individual droplet. The droplets containing the targeted sequence, will be amplified and a TaqMan reporter dye will release a fluorescent signal (Bio-Rad). To then generate the results, the samples are amplified to endpoints in a conventional thermal cycler followed by a droplet reader device counting PCR-positive and -negative droplets with a detector. The droplet reader is connected to a computer software for further analysis (Bio-Rad).

1.8 Flow Cytometry

Flow cytometry is a laser-based technology that will detect single cells based on their chemical and physical properties. Flow cytometry is performed using an instrument called a flow cytometer. In the instrument, the signal will then be detected and measuring using single or multiple lasers (McKinnon, 2018). The detectors are of two sorts, forward scatter detector (FSD) and side scatter detector (SSD). The total quantity of FSD correlates to the size of the cell and the SSD is proportional to the granular, complexity and fluorescent content of the cell. These detectors can alone distinguish cell populations (McKinnon, 2018).

For detection of specific types of cells, the samples can be prepared for fluorescence measurement by staining with fluorescent dyes and fluorescently conjugated antibodies specific for surface molecules on the cells and dyes.

Fluorescence-minus-one (FMO) control is a mixture of all the conjugated antibodies used in the staining process except the one relative to the antibody that is being controlled. The FMOs are much needed because it allows for deciding the flow gating and the influence of the other fluorochromes under the analysis (Ortolani, 2022).

Compensation is also needed for flow cytometry. It refers to the process of correcting for fluorescence spillover, which means removing the signal of any given fluorochrome from all detectors except the one devoted to measuring that dye. It is necessary to be able to differentiate between populations of cells (Tung et al., 2007).

1.9 Aims of the Thesis

The primary objective of this study was to study the effect of knockout of *Adenosine Deaminase 2 (ADA2)* and knock in of *ADA2* R169Q mutation on the activity and expression of the *ADA2* gene and study the impact of *ADA2* downregulation on T-cells functioning using CRISPR/Cas9. The editing on T-cells is done to understand more of the mechanism of the deficiency of Adenosine Deaminase 2 (DADA2).

The project is divided into two aims:

Aim 1 – effectively knock out *ADA2* and knock in R169Q mutation in T-cells. Evaluate editing efficiency NHEJ and HDR editing using ddPCR, evaluate *ADA2* activity and evaluate loss of *ADA2* transcript using qPCR.

Aim 2 – studying the effect of *ADA2* knockout and R169Q mutation on T-cells using flow cytometry in T-cell activation and proliferation downstream assays. Done with different donors with WT samples (short culturing), WT samples + R169Q + KO (long culturing, 10-14 days).

2 Materials and methods

2.1 Materials

T-cells were enriched from buffy coats. Buffy coats were collected from healthy blood donors, provided by the Blood Bank at Oslo University Hospital HF, Rikshospitalet, Oslo, Norway with ethical approval and consent for research.

Complete lists of reagents, equipment, software, and instruments used in this project are listed in appendix I.

Donor information: 2 donors:

1. Donor: female, 57 y/o
2. Donor: male, 32 y/o.

2.2 Designing PCR Primers

For both *ADA2* knock-out (KO) and *ADA2* knock-in (KI) of R169Q, pre-designed probes were employed, which included the *ADA2*-specific single guide RNA (sgRNA) #3 for the electroporation step and a set of probes consisting of forward and reverse primers and a non-homologous end joining (NHEJ) probe, shown in table 2.1 and 2.2. The design of probes are shown in figure 2.1 and 2.2.

The Snap Gene software (from GSL Biotech, available at snapgene.com), was used for making the remaining probes for KO AND KI. A repair template was designed to facilitate the knock-in (KI) of the R169Q mutation in the Adenosine Deaminase 2 (*ADA2*) gene, with a total length of 100 base pairs (bp). The repair template was engineered to contain a single nucleotide polymorphism (SNP) at the site of the desired mutation and a specific base change from cytosine (C) to thymine (T) to generate the R169Q (p. Arg169Gln) mutation sequence. HDR R169Q probe was made with added SNPs for reliable detection of editing, and a single nucleotide base change from C to T for R169Q mutation. Used already designed *ADA2* gRNA #3, forward, reverse and *ADA2* NHEJ probe.

Single-nucleotide polymorphisms (SNPs) are differences that occur at a single position in different individuals in the DNA sequence. SNPs are used in designing CRISPR probes and

can serve as a marker for a particular trait, which allows for more precise targeting of specific genomic loci (Chen et al., 2020).

Prior to the project, the laboratory evaluated various guide RNAs (gRNAs) for editing the *ADA2* gene in PBMCs and assessed their performance (figure 2.1). Based on the results, it was observed that gRNA #3 demonstrated the best performance in healthy donor (HD) PBMCs and was in closest proximity to the cutting point compared to other gRNAs evaluated. *ADA2* gRNA #3 showed to have the best performance in the HD PBMCs and was closest to the cutting point compared to the other gRNAs tested. Thus, gRNA #3 was identified as the optimal candidate for this project. This approach was selected based on its ability to achieve precise editing of *ADA2* in PBMCs, which is crucial for the accurate investigation of *ADA2*'s effects on T-cell function.

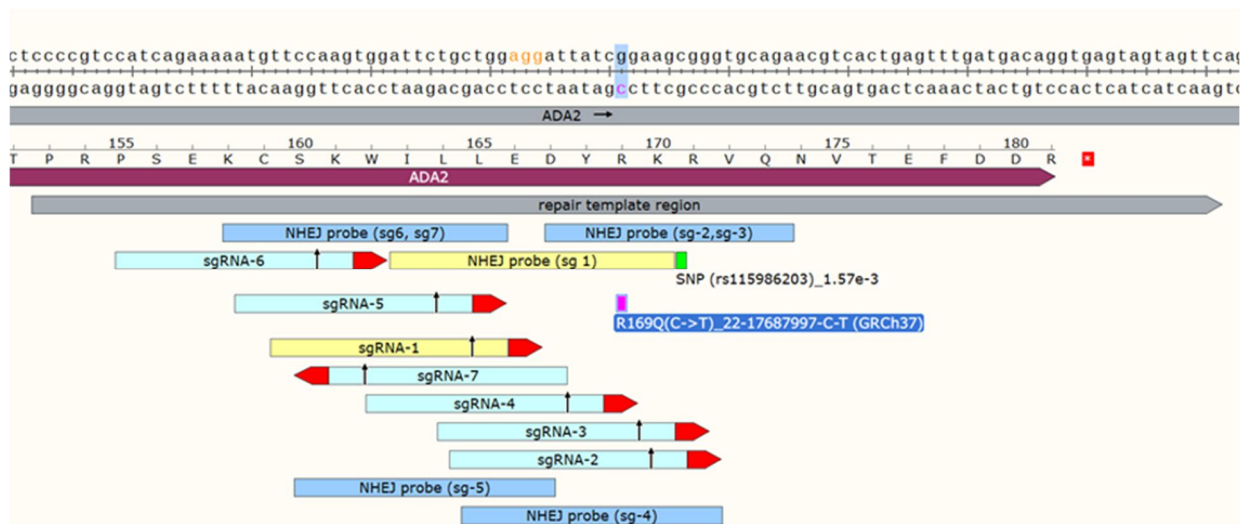


Figure 2.1: snapshot of gRNAs evaluated in the laboratory for editing of the *ADA2* gene in PBMCs

gRNA #3 showed to have the best performance in the HD PBMCs and was closest to the cutting point compared to the other *gRNAs* tested. NHEJ probe (sg-2, sg-3) marked in blue was used as the NHEJ probe during the project. Marked in pink, is the *ADA2* R169Q point mutation. PAM sequence is marked in yellow. The design was made using the Snap Gene software (GSL Biotech) by another laboratory member.

Table 2.1: showing the RNP mix sequences used in editing of ADA2.

Mutation shown in pink, PAM sequences shown in blue, and SNPs shown in green.

ADA2 sgRNA #3	TGCTGGAGGATTATCGGAAG CCG
ADA2 repair template (ssODN) forward (R169Q mut)	CCCCGTCCATCAGAAAAATGTTCCAAGTGGATT CTGCTGGAGGACTACA ^{AA} AAGCGGGTGCAGAACGTC ACTGAGTTTGTATGACAGGTGAGTAGTAGTTC

Table 2.2: showing the probes used for digital droplet PCR.

For R169Q HDR probe: mutation shown in pink, and SNPs shown in green. The additional probes were already designed probes established in the group.

Primer name	Templates used in sequence building (5' to 3')	Temperature °C
ADA 2 Forward probe	GGTGAGGAATGTCACCTACA	57,3
ADA 2 Reverse probe	GTACCAAGGGAGACACCTAC	59,4
ADA 2 Reference probe	GCCACATCTGTTTCACCCCA	59,4
ADA 2 NHEJ WT probe	ATTATCGGAAGCGGGTGCAGA (WT->SNP)	60
ADA2 R169Q HDR probe	CTGGAGGACTACA ^{AA} AAGCGG (WT->R169Q)	61,8

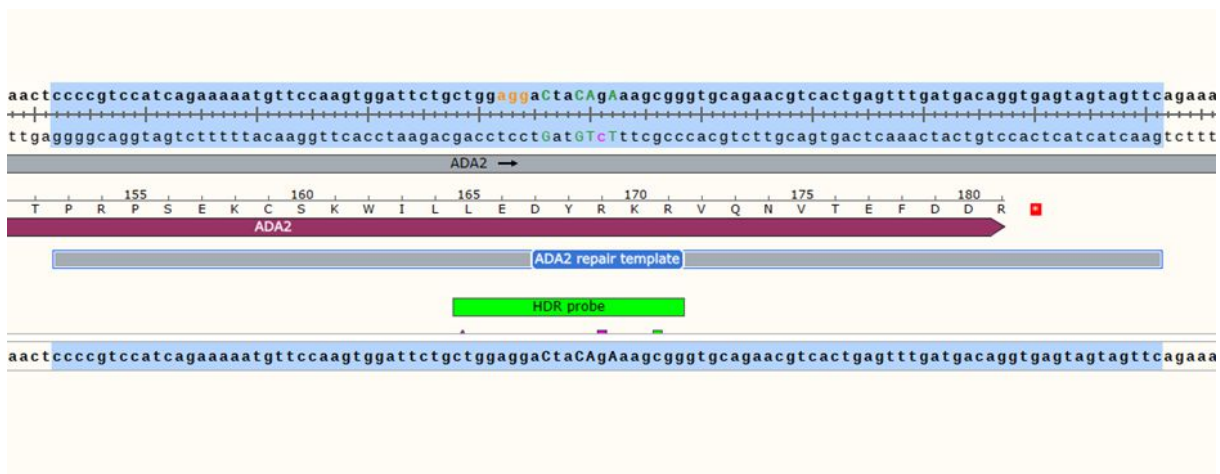


Figure 2.2: snapshot of probe designs for ADA2 R169Q knock-in mutation.

Snagene file including the design of ADA2 R169Q mutation repair template and HDR probe for R169Q. PAM sequence is marked in yellow, mutation marked in pink and SNPs in green. The sequences were designed using the Snap Gene software (GSL Biotec).

2.3 PBMC work: *ADA2* Gene Editing of Human PBMCs

2.3.1 Cultivation of Peripheral Blood Mononuclear Cells (PBMCs)

All work was done in a sterile BL-2 laminar hood. The previously isolated Peripheral Blood Mononuclear cells (PBMCs) were transferred from -150 °C freezer on dry ice. They were thawed in a 37 °C water bath for approximately 2 minutes, before they were added into 10 ml pre-warmed thawing medium (T-cell Expansion Medium (appendix I, table 1). The cells were centrifuged (1400 rpm, 5 min) at RT and the pellet was resuspended first in 1 ml pre-warmed T-cell expansion medium with added 1X Penicillin-Streptomycin (P/S), 15 µl/ml anti-human CD3/CD28, 120 U/ml Recombinant Human IL-2 (IL-2), 3 ng/ml IL-7, 3 ng/ml (appendix I, table 1), before adding additional 9 ml media. The volume of the T-cell expansion medium enriched with CD3/CD28 (Stemcell Technologies, #10970) was then adjusted to acquire 1 M cells/ml final concentration. Cells were then seeded into T175 cell culture flasks for T-cell expansion and placed in the incubator at (37 °C, 5% CO₂) for 72 hours.

In the first runs of experiments Gibco™ RPMI 1640 Medium with added Fetal Bovine Serum (appendix I, table 1) was used, before switching to Immunocult T-cell Expansion Medium (appendix I, table 1), to get better cell growing rate.

The cytokines IL-2, IL-7 and IL-15 select and activate the T-cells that we want to keep. 90% of electroporated cells are CD4⁺ and CD3⁺.

Cell counting was done using Countess (Thermo Fisher Scientific, MA, USA), by mixing 10µl of cells and 10µl of Trypan blue cell counting dye (Thermo Fisher, MA, USA #C10228).

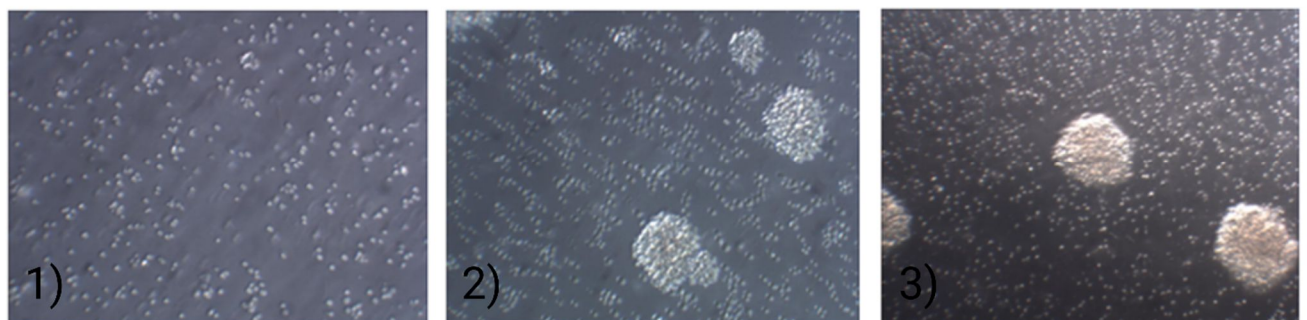


Figure 2.4: microscopy photos of cultivated PBMCs.

1) Photo taken shortly after the cells were seeded into a culture vessel and allowed to adhere and begin to proliferate. T-cells grows in clusters upon activation, as seen in photo 2) and 3), taken on day 4 and 6 after cultivation. Photos taken using GXCAM camera with the GXCapture™ software and microscope.

2.3.2 Electroporation

Preparation of electroporation mix, Ribonucleoproteins (RNPs) complexes

100 pmol (= 1 μ l) *ADA2* annealed crRNA guide 3 (100 μ M stock, IDT) and 61 pmol Cas9WT protein (IDT) were added by pipetting into a 96 well plate. The plate was then sealed, spun down and incubated (RT, 15 min), and placed on ice prior to adding the repair template. Repair template is not added until cells are ready for electroporation since it can degrade the ribonucleoprotein (RNP) complexes.

100 pmol of *ADA2* FWD unmodified repair template (100 μ M stocks, IDT Ultramer oligo) was added to the RNP complexes. The plate was then sealed again and spun down. The plate was kept on ice until the cells were ready for the electroporation procedure.

Preparation of cells for electroporation

The cells were harvested and counted by taking an aliquot, to achieve 1 million cells per sample. The cells were centrifuged (1400rpm, 5 min), before the pellet was resuspended in 1 ml pre-warmed (37 °C) Phosphate-buffered saline (PBS). An additional 10 ml pre-warmed PBS was added, prior to centrifugation (1400rpm, 5 min).

Electroporation step

Electroporation was performed using the Lonza 4D Nucleofector System, Core Unit (Lonza Cat. no. AAF-1002B) with a 16-well Nucleocuvette™ Strip and 4D-Nucleofector 96-well Unit.

The prepared cell-pellet was resuspended in MaxCyte electroporation buffer (1 M cells in 20 μ l buffer per sample), before pipetting the cell suspension into the 96 well plate containing the previously prepared RNP mix. The samples in the 96 well plate were transferred to a Lonza 16-well electroporation strip and placed into the Lonza electroporation system.

Table 2.3: program used during electroporation step on the Lonza 4D Nucleofector System.

Electroporation program	
Solution	Primary Cell P3
Pulse code	EO-115

After the electroporation was complete, 85 μ l of pre-warmed T-cell recovery medium (Immunocult™-XF T-cell Expansion Medium (StemCell Technologies, #10981) supplemented with IL-2 (Recombinant Human IL-2, Peprotech, # 200-02) at 250 U/ml) without P/S was added into each well of the 16-well strip, and the strip was placed in incubator (37 °C,

15 min.) The electroporated cells were added to a previously prepared 24-well plate with each well containing 350µl pre-warmed T-cell expansion medium without P/S. 100 µl media was added to the 16 strip to wash out excess cells and added to the designated wells. 1 ml of PBS was added to the empty wells to avoid evaporation. The cell culture plate was then placed in the incubator to rest overnight (37 °C, 5% CO₂).

The following day, P/S was added to the wells after cell counting. A recovery medium was added to ensure the cells did not exceed 2M/ml. The media change was repeated two days after adding P/S.

1 M cells per sample was harvested 4 days after electroporation for downstream analyses.

2.4 DNA Isolation

Purification of DNA was carried out following the DNeasy®Blood & Tissue gDNA extraction Kit (QIAGEN, DEU).

1 M cells per sample was centrifuged (7500 rpm, 10 min), and the supernatant discarded. Next, the subsequent steps in the manufacturer's protocol, given in appendix I, table 1, were followed. In short, the cell pellet was resuspended in ATL buffer, followed by cell lysis and degrading DNA-associated proteins by adding proteinase K. Then AL buffer was added, which contains a chaotropic salt that makes DNA bind to the silica membrane of the spin column. Ethanol was then added, to cause DNA to separate from the cellular debris because DNA being insoluble in the presence of alcohol and salt. Wash buffers AW1 and AW2 (containing alcohol) were added to remove contaminants. AE elution buffer (low salt buffer) was added to elute the purified DNA.

2.5 Qubit

The DNA extraction was followed by Qubit™ dsDNA HS Assay Kit using Qubit 4 Fluorometer (Thermo Fisher, MA, USA) for precise quantification of double stranded DNA (dsDNA). The calculations are further used for calculating amount of DNA in the samples and ddH₂O needed for diluting the samples.

The standards and reagents used had to equilibrate to reach RT before use. For each experiment, new standards were performed for new calibration. For each sample, the

following volumes were mixed to a Qubit™ Assay Tube: 199µL Qubit™ Working solution + 1µL sample. For the standard: 190µL Qubit™ Working solution + 10µL standard. The tubes were further vortexed 2-3 seconds before incubation (RT, 2 min). For measurement on the Qubit® Fluorometer, program for dsDNA was selected with an input volume of 1 µl for the DNA samples. Before reading the samples, the two standards were read. The calculations done by the Qubit® Fluorometer, are the original DNA concentration in each sample in ng/µl.

2.6 Digital Droplet PCR (ddPCR)

Table 2.4: showing the calculations for primer-probe mix for either NHEJ or HDR. The calculations are done for 1 sample.

Primer-Probe Mix (NHEJ)/(HDR)	For 100 µl
MilliQ H ₂ O	54 µl
Primer fwd	18 µl
Primer rev	18 µl
NHEJ or HDR probe (FAM)	5 µl
Reference probe (HEX)	5 µl

Table 2.5: showing the calculations for master mix for either NHEJ or HDR. The calculations are done for 1 sample.

Master Mix (NHEJ)/(HDR)	For 1 sample
ddPCR Supermix (no dUTP)	10 µl
Primer-Probe Mix (NHEJ)/(HDR)	1 µl
MilliQ H ₂ O	1 µl

The ddPCR master mix for non-homologous end joining (NHEJ) and homology-directed repair (HDR) were prepared according to table 2.4 and 2.5. The DNA concentrations of the samples from DNA purification was normalized to 4 ng/µL in 20µL. In a ddPCR semi skirted 96 well plate, 12 µl of the HDR and NHEJ master mixes were added to the designated wells designated together with 8 µL of the normalized DNA sample. The 96 well plate was loaded into the Automated Droplet Generator #1864101 (Bio-Rad, CA, USA) before the plate was transferred to a T100 Thermal Cycler (Bio-Rad, CA, USA) with the following program set:

<i>Temperature (°C)</i>	<i>Time</i>	<i>Cycles</i>
95	10 min	
94	0.30 sec	42 x
56	3 min	

98	10 min	
4	∞	

After the PCR program, the PCR 96 well plate was placed into the QX200 Droplet Reader (Bio-Rad, CA, USA), which analyzes each droplet individually using a two-color detection system that is set to detect FAM and HEX. The Droplet Reader is connected to QuantaSoft software. In the QuantaSoft the following plate-reader parameters were defined:

Experiment	RED
Supermix	ddPCR Supermix for Probes (no dUTP)
Target1, Type	Ch1 Unknown
Target1, Type	Ch2 Unknown

This two-channel assay used FAM dye and one HEX dye. The droplets will consequently be grouped into one of four clusters: double-positive (orange, droplets that contain both target sequences and emit both HEX and FAM fluorescence), FAM-positive (blue), HEX-positive (green), and double-negative (grey, empty droplets without any amplifiable template that do not emit fluorescence in either channel).

Once the droplet reading was done, the data was gated and analyzed in QuantaSoft using a 2D Amplitude plot.

The values were further calculated in Microsoft Office Excel. To obtain the percentage of HDR, the amount of FAM+/HEX+ positive droplets was divided by the total amount of droplets with probes. The overall percentage of total NHEJ probe drop-off rate was calculated by dividing the amount of FAM-/HEX+ positive droplets by the total amount of droplets with probes. To obtain the percentage of NHEJ, the HDR percentage was subtracted from the total NHEJ drop-off percentage for each sample.

2.6.1 Statistical Analysis

Statistical analysis was done using Microsoft Excel or GraphPad Prism 9 (GraphPad Software).

2.7 ADA2 Activity Test in CRISPR/Cas9 ADA2 Knock Out and WT PBMCs using Diazyme Kit

2.7.1 Lysis of the cell

4 days after electroporation of the PBMCs, cell pellets and medium (supernatant) (for approximately 3 M cells) were collected in separate tubes and on ice. The pellets then were lysed with 100 µl Pierce™ RIPA lysis and extraction buffer (89900, Thermo Fischer), with 100x PIC (1:100) (Halt™ Protease Inhibitor Cocktail). The cell lysis mixture was rotated for 15-30 minutes in a cold room and then centrifuged (14 000g, 15 min) 4 °C. Cleared supernatants were stored at -80 °C for downstream analysis.

To concentrate media samples, 500 µl of the media were filtered through 10kDA filter membrane (Pierce™ Protein Concentrator PES, 10K MWCO, 20-100 ml, 88535, Thermo Fisher, MA, USA) by centrifugation (12 000g, 5 min) at 4 °C. Concentrated samples were collected from the top of the filter and stored at -80 °C.

2.7.2 BCA assay

The total level of protein was determined in the cell lysates and media using Pierce™BCA Protein Assay (Thermo Fisher Scientific, MA, USA).

10 µl of concentrated media and lysed cells, diluted in 1:10 RIPA buffer, were added by 200 µl working buffer in each well of a 96 Well Black/Clear bottom well Plate. The plate was then placed on a plate shaker for 30 seconds and incubated (37 °C, 5% CO₂) for 30 minutes before measuring the absorbance at 580 nm using Infinite® M Nano, single-mode microplate reader, monochromator optics (Tecan, CH). The working reagent and protein standard were prepared according to the manufacturer's instructions.

2.7.3 Activity test in PBMC using Diazyme kit.

ADA2 activity was measured by using the Adenosine Deaminase Assay kit (Diazyme Laboratories, Poway, USA). The Diazyme ADA2 kit used in this project is a colorimetric assays, utilizing colorimetric substrates that forms a chemical reaction with ADA2, and results in colored product, where the intensity of the color then is measured spectrophotometrically at the specific wavelength of 556 nm for quantifying ADA2 enzyme activity.

This assay is designed based on the deamination of the nucleoside adenosine to inosine, which then again turns into hypoxanthine by purine nucleoside phosphorylase (PNPase). The hypoxanthine is then by xanthine oxidase, converted to hydrogen peroxide and uric acid. The hydrogen peroxide reacted with N-Ethyl-N-(2-hydroxy-3-sulfopropyl)-3-methylaniline (sodium salt) and 4-aminoantipyrine (ampyrone) with peroxidase to create a quinone dye, which has a maximal absorbance of 556 nm.

ADA2 enzyme activity was measured for the previously prepared *ADA2* edited T-cells (section 2.3.2). To inhibit the *ADA1* enzyme activity, samples were first incubated with erythro-9-(2-hydroxy-3-nonyl) adenine (EHNA) at the final concentration of 17.5 μM for 5 min at 37 °C. Control samples were prepared without EHNA in parallel. Samples and protein standards (provided by the kit) were then equilibrated with 180 μl Reagent 1 (provided by the kit) at 37 °C and then the initial absorbance was measured at 556 nm (A1), 3 min after adding R1 Reagent. Reagent 2 (R2; 90 μL) was added to start the reaction, during which the absorbance was recorded at 556 nm every 10. minute for 4-8 hours to establish an optimal endpoint read (A2) at 180 min. Plate reader used: Infinite® M Nano, single-mode microplate reader, monochromator optics (Tecan, CH).

The Calibrator 50 (Cal50) is a standard solution that is included in the Diazyme *ADA2* enzyme activity kit. Cal50 with 0.9% saline solution (sodium chloride and ddH₂O) was used as reference standard to establish a calibration curve which allows quantification of *ADA2* enzyme activity in unknown samples. Cal50 has a known concentration of *ADA2* enzyme activity and is utilized for generating a standard curve by plotting its absorbance values against its known concentration. The absorbance values of unknown samples are then compared to the standard curve to determine their *ADA2* enzyme activity levels.

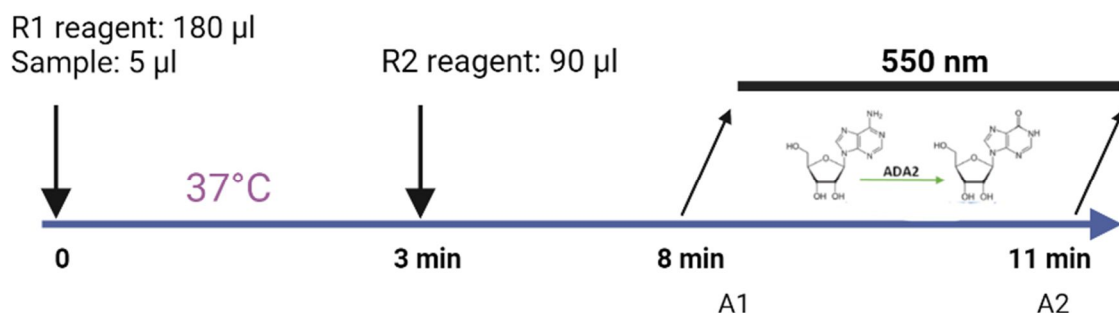


Figure 2.5: illustration of the assay procedure for the Diazyme ADA2 (Adenosine Deaminase 2) Activity Test.

The figure illustrates the assay procedure of the diagnostic test used to measure *ADA2* enzyme activity in patient samples, Diazyme *ADA2* activity test. This assay is designed based on the deamination of the nucleoside adenosine to hydrogen peroxide

which reacts with *N-Ethyl-N-(2-hydroxy-3-sulfopropyl)-3-methylaniline (sodium salt)* and *4-aminoantipyrine (ampyrone)* with peroxidase to create a quinone dye, which has a maximal absorbance of 556 nm. The figure is made by an author using Biorender, based on figure from ADA2 Diazyme kit.

2.8 Evaluation of Downregulated *ADA2* Transcription

2.8.1 RNA isolation

Isolation of RNA was done using the Total RNA Purification Kit (Norgen Biotek Corp., Canada), as described by the manufacturer. In short, the provided 350 µl RL buffer was added, and the lysis mix vortexed for 15 sec before adding 200 µl 96-100% ethanol to the lysate, and again vortexed for 10 min. The lysate was added to a RNeasy column and centrifuged (14 000 rpm, 1 min.) The flow through was discarded before placing the spin column into the same collection tube. The bound RNA was then washed to remove any remaining impurities using the provided Wash Solution A. This step was repeated three times. The purified RNA was then eluted with the provided Elution Solution A.

Prior to the extraction, all the equipment used was cleaned by using RNase Away™ Decontamination Reagent (Thermo Fischer Scientific). The resulting RNA was used as the template for cDNA synthesis.

2.8.2 cDNA synthesis

The cDNA was prepared from 0.2µg RNA input by using the SuperScript™ VILO™ cDNA Synthesis Kit (Thermo Fisher Scientific, MA, USA).

Calculated volumes of 5X VILO™ Reaction Mix (4 µl per reaction) and 10X SuperScript™ Enzyme Mix (2 µl per sample) were first prepared as a master mix. RNA samples (200ng) and NFW (Nuclease-Free water) (calculated and added to get 20 µl in total) were further added in PCR 8-Well Tube strips up to the final volume of 20 µl. cDNAs were generated in the T100 Thermal Cycler (Bio-Rad, CA, USA) with the following program set:

<i>Temperature (°C)</i>	<i>Time</i>	<i>Cycles</i>
25	10 min	1
42	120 min	1
85	40 min	1

8-Well Tube strips got span down before continuing onto Real-time quantitative RT-PCR.

2.8.3 Real-time quantitative RT-PCR

The Real-time quantitative PCR (RT-PCR) reactions were carried out using the SsoAdvanced™ Universal SYBRGreen Supermix kit (Bio-Rad, CA, USA), on CFX Opus 96 Real-Time PCR system (Bio-Rad, CA, USA). The reaction master mix was prepared by mixing SsoAdvanced™ Universal SYBRGreen Supermix (10 µl per reaction), *ADA2* forward primer (5µM) (0,3 µl per reaction), *ADA2* reverse primer (5µM) (0.3 µl per reaction) and RFW (7,4 µl per sample). RNA samples were first diluted 1:10 with RFW, and 9 µl was added to 18 µl of the master mix in corresponding wells of a 96 qPCR well plate.

Non-template control (NTC) sample was prepared by adding NFW only to the corresponding well. The 96 qPCR well plate was transferred to CFX Opus 96 Real-Time PCR system (Bio-Rad, CA, USA) and ran on qPCR program:

<i>Step</i>	<i>Temperature (°C)</i>	<i>Time</i>	<i>Cycles</i>
	50	2 min	1
<i>Initial denaturation</i>	95	10 min	1
<i>Denaturation</i>	95	15 sec	
<i>Anneal/extend</i>	60	1 min	40
<i>Melting curve</i>			
<i>Denaturation</i>	95	15 sec	
<i>Anneal/extend</i>	60	15 sec	

The CFX Maestro (Bio-Rad, CA, USA) software was utilized for analyzing data after the qPCR run. For controlling data, the human housekeeping gene *ss18* was used as a reference gene.

Gene expression was calculated by double delta Ct analysis. The mean threshold cycle (Ct) values were subtracted from the reference gene from the targeted gene $\Delta CT = CT$ (a target gene) $-CT$ (a reference gene). This method yields the fold change of the expression of the targeted gene in a target sample when it is compared to the reference sample (*ss18*), after normalization to a reference gene.

2.9 Flow Cytometry and Fluorescent Staining of T-cells

Flow cytometry allows for rapid analysis of a high number of cells. The analysis is achieved by passing one cell at a time through one or more lasers. When the lasers hit the cells, the amount of light that will scatter and produce fluorescent light signals will be detected and will say something about the characteristics of the cells. The technique is a beneficial tool in analyzing T-cell functions including proliferation, cytotoxicity, survival, and cell signaling (Chattopadhyay & Roederer, 2010).

2.9.1 Pre-stimulation for activation and proliferation assays

The previously electroporated cells for *ADA2* knockout and *ADA2* R169Q reagents (section 2.3.2) were cultured in Immunocult™-XF T-cell Expansion Medium supplemented with IL-2 for 10 days before continuing with downstream T-cell functioning assays.

The cells were first treated by DNase (Deoxyribonuclease). The treatment will reduce cell clumping which is necessary since a single-cell suspension is critical for successful isolations and to not hinder labeling of the targeted cells.

50 µl DNase/ml with a concentration of 1000 ug/µl were added to the cell samples suspended in 1 ml Immunocult™-XF T-cell Expansion Medium with 120U/ml IL-2. The samples were incubated at 37 °C in water bath for 30 min and washed with extra 4 ml medium, before resuspension and cell counting. Cells were added by calculated volume of media to achieve a desired concentration of 1M cells/ml. Cells being used for activation assay were seeded 100µl per well (100 000 cells) into a Falcon® 96-well Clear Round Bottom Plate (Corning Inc., MA, USA #351177). Cells for proliferation assay were stained with carboxyfluorescein succinimidyl ester (CFSE) dye using the CellTrace™ CFSE Proliferation Kit (Thermo Fisher Scientific, MA, USA) before seeding.

CFSE staining for proliferation assay

For T-cell proliferation measurement to get visualization of generations of proliferating cells, the CFSE dye was applied using the CellTrace™ CFSE Cell Proliferation Kit, for flow cytometry (Thermo Fisher Scientific, MA, USA). The CFSE staining was done after DNase treatment before the stimulation step. The CFSE stained cells were measured with flow cytometry for monitoring proliferation within the populations of stimulated cells. Cells stained with CFSE can be used for this since it distributes the dye equally when they divide.

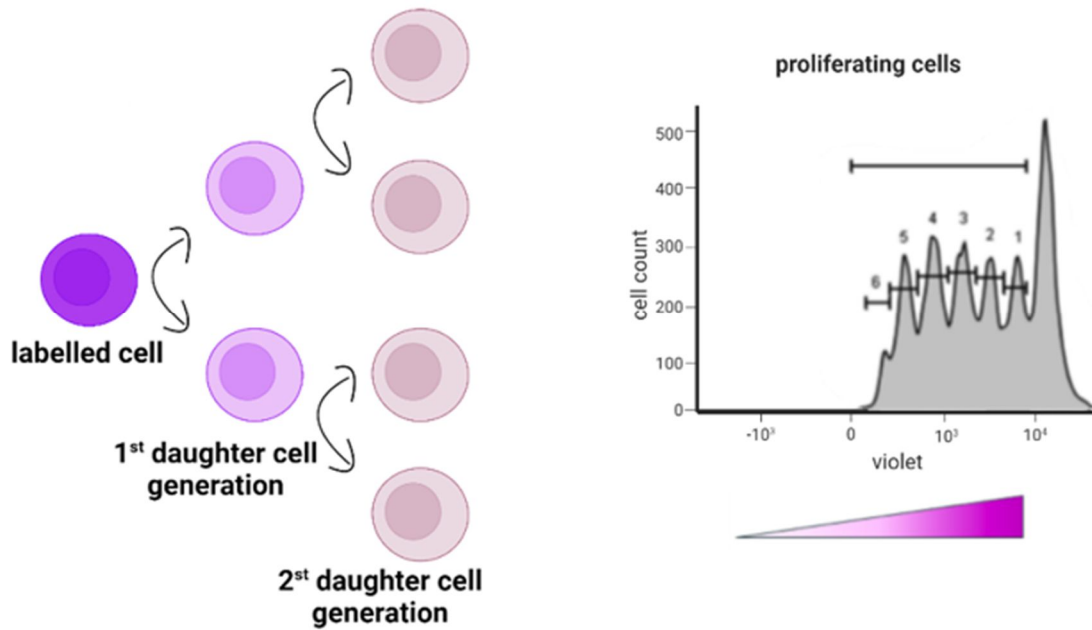


Figure 2.6 Visualization of the division of cells using CFSE dye.

The CFSE binds intracellular amines and is diluted by the division of the cell. As the dye evenly dilutes into the daughter cells in cell division, each round of cell division can be tracked individually over time as seen in the graph.

After the DNase treatment, CFSE was prepared fresh by adding 18 μ l Dimethyl Sulfoxide (DMSO) to the CellTrace™ CFSE (lyophilized powder) tube. The CFSE was diluted in PBS (1:2000) for cell suspensions at the concentration of 1M/ml. The cells were resuspended in 1 ml CFSE/PBS mix per 1 ml cell suspension and incubated in 37 °C water bath for 20 minutes, shaking the tubes in circles every 5. minute. Cold medium up to 5x volume were added to stop the staining process during 5 min incubation at RT. The cells were centrifuged (400xg, 6 min), followed by washing the cells once with PBS and once with media, before resuspending the pellet in 2 ml media. The cells were counted using Countess® (Thermo Fisher Scientific, MA, USA), adjusted to 1 M/ml and seeded at 100 μ l (100 000 cells) per well in 96 Well Round (U) Bottom Plate.

The cells were then incubated (37 °C, 5% CO₂) for at least 4 hours before stimulation.

2.9.2 Stimulation of T-cells for activation and proliferation assays

For the proliferation plate, the cells were stimulated 4 hours post CFSE staining and were then incubated for 5 days prior to the antibody staining.

For the activation plate, the cells were stimulated directly after seeding. The cells were stimulated at 48 hours and 24 hours prior to antibody staining.

For stimulation of the cells in both immunoassays the stimulants CD3 Monoclonal Antibody (OKT3) (Thermo Fisher Scientific, MA, USA), CD28 Monoclonal Antibody (CD28) (Thermo Fisher Scientific, MA, USA), Phytohemagglutinin-L (PHA-L) (Roche, CH) and Dynabeads™ Human T-Activator CD3/CD28 (Thermo Fisher Scientific, MA, USA) were used, including unstimulated wells as controls.

The stimulants were diluted in the Immunocult™-XF T-cell Expansion Medium with IL-2, and added to the cells according to these calculations:

- Monoclonal soluble Antibodies CD3/CD28: final concentration of 200g/ml.
- Dynabeads™ Human T-Activator CD3/CD28: 1:2 bead to cell ratio.
- PHA-L: concentration of 1µg/µl. Diluted the PHA 1:10 in PBS.

The stimulants used in the assays are presented in appendix I, table 1. A full list of the antibodies used in the assays are listed in appendix I, table 2 and 3.

2.9.3 Antibody staining

Cells were transferred to the Nunc™ 96-Well Polystyrene Conical Bottom MicroWell™ Plates (Thermo Fisher Scientific, MA, USA, # 249570)), and washed once with 200 µl FACS buffer (PBS, 2% FBS) at 400xg for 6 min and then resuspended in 25 µl FACS. The plate was stored on ice between the washing steps. FVD660 was mixed in FACS (1 µl FVD660 in 1500µl FACS), before adding it to the fluorescent antibody mix. Fluorescence Minus One (FMOs) control were made to be able to accurately identify positive events in the samples. FMOs were made by making mixes of all antibodies except for the one of interest.

For each activation experiment, we employed FMO controls to account for CD3, CD4, CD8, CD25, and CD69, which also included unstimulated controls.

For the proliferation assays, FMO controls for CD3, CD4 and CD8 were used. Including cell controls without stimulation and controls without staining with CFSE.

The cells were mixed with the antibodies at appropriate dilutions and incubated in the dark at 4 °C for 30 minutes.

After incubation the plate were spun at 400xg for 6 minutes and washed twice with 150 μ l and 200 μ l FACS, and then resuspended in 40 μ l FACS before analysis with the flow cytometer.

Preparation of Compensation beads

To gate parameters for obtaining accurate fluorescence signal, UltraComp eBeads™ (Thermo Fisher, MA, USA, #01-2222-41) were used. One droplet of the bead mixture was mixed with 1,5 μ l of each type of antibody and are then incubated at 4 °C for 30 minutes before adding it to the plate.

UltraComp eBeads™ consist of two groups: a positive population that can bind to antibodies from mice, rats, or hamsters, and a negative population that does not interact with antibodies. Upon the addition of a fluorochrome-conjugated antibody to the beads, both the positive and negative populations will be detected.

For the compensation analysis, a sample of the cells stained with FVD660 containing 50% live cells was included. This was done by taking a small aliquot of the cells, heating it at 65 °C for 15 minutes and placed on ice for 1 minute. The heat-killed cells were subsequently added back to the well, to make a 1:1 live: dead cell sample.

2.9.4 Flow cytometry

The flow cytometry analysis was done with iQue® 3 Advanced Flow Cytometry System (Sartorius AG, DE, #91377).

The assay was designed according to the panel in figure 2.6 and 2.7.

Analysis of data was done by FlowJo v10 (Becton Dickinson).

Table 2.6: Antibody panel for T-cell activation assay

The table presents an antibody panel designed for flow cytometry analysis, specifying the antibodies used for immunophenotyping or detection of specific cell populations or markers.

	445/45	530/30	572/28	615/24	673/30	780/60
405	CD4 BV421		CD28 BV570			CD69 BV786
488				CD25 PE- CF594		
640					FVD660	CD3 APC Fire750

Table 2.7: Antibody panel for T-cell proliferation assay

The table presents an antibody panel designed for flow cytometry analysis, specifying the antibodies used for immunophenotyping or detection of specific cell populations or markers.

	445/45	530/30	572/28	615/24	673/30	780/60
405	CD4 BV421			CD3 BV605		
488		CFSE				CD8 PE-Cy7
640					FVD660	

The cells were cultivated for different lengths. The assays done on WT T-cells only, were thawed and stimulated on the same day, and went through T-cell staining and flow analysis 48 hours after post stimulation for activation assay. For proliferation assay the identical principles as the activation assay was followed, with the distinction being the incorporation of staining and flow analysis at a time point of 96 hours after the stimulation event. With a total of 3 or 6 days in culture.

For the assays done on edited T-cells, the cells got stimulated 10 days post EP, and stained and analyzed 48 hours after for activation, and 6 days later for proliferation assay. With a total of 12 or 16 days in culture.

The two sets of cultivation methods are further described as short and long cultivation assays.

3 Results

3.1 ADA2 Editing in T-cells

The peripheral blood mononuclear cells (PBMCs) utilized in the electroporation protocol were obtained from a total of two human donors, M32 (donor 1), F57 (donor 2). The delivery of RNP complexes, referring to RNP mix, was successfully done by electroporation. After completing droplet analysis, the acquired data was gated and further analyzed using QuantaSoft software, utilizing a 2D Amplitude plot for visual representation, as depicted in figures 3.1-3.4.

For estimating the experiments measuring NHEJ events, the X-axis present the amplitude from channel 2 with HEX, and the Y-axis present the amplitude from channel 1 with FAM. The HEX+/FAM+ subpopulation, binding both FAM and HEX labeled probes, indicated both the DNA marker probe and NHEJ probe were able to bind to the DNA, which in turn means that no indels were introduced to the sequence. This observation suggests that the DNA sequence remained unaltered, indicating the absence of NHEJ repair mechanism. The HEX+/FAM- subpopulation, characterized by binding of the HEX-labeled probe and negligible or weak binding of the FAM-labeled probe, where FAM probe would not be able to bind to the targeted site in presence of an indel, indicates the presence of NHEJ-mediated DNA repair.

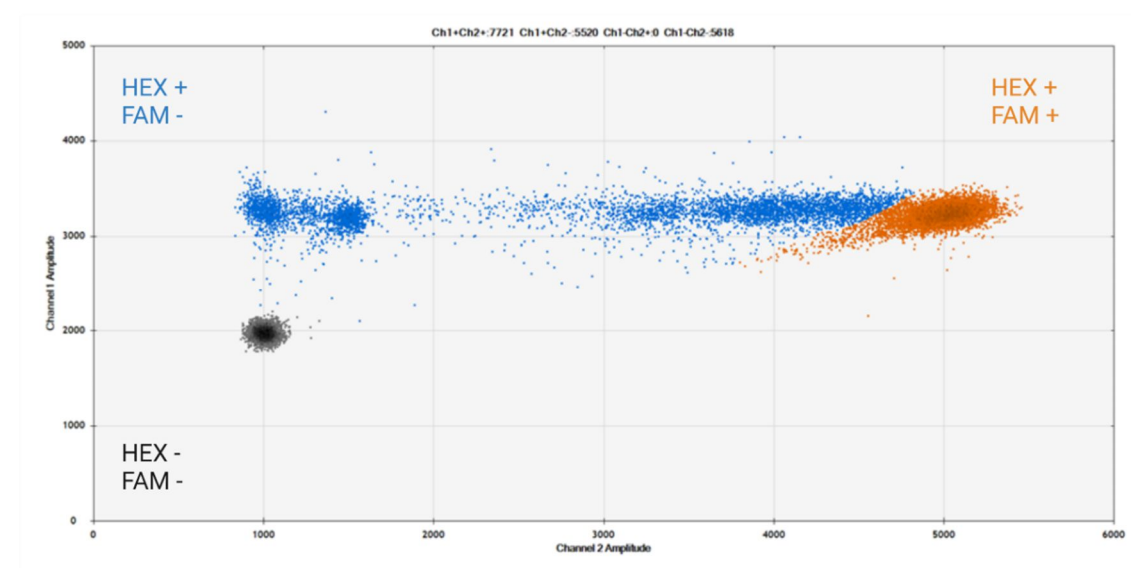


Figure 3.1: NHEJ gating of ADA2 PBMCs in a 2D amplitude plot.

The plot shows a 2D Amplitude plot where the amplitude of channel 1 fluorescence (FAM-NHEJ probe) is plotted against amplitude of channel 2 (HEX probe). It shows a two-dimensional cluster in which channel 1 amplitude fluorescence (NHEJ probe, FAM) is plotted against channel 2 amplitude (Reference probe, HEX). The grey dots are droplets with no probes attached, and the orange dots are HEX positive (meaning that it has bounded with DNA marker probe), and FAM positive (meaning NHEJ probe was able to bind to the DNA, which again means that there was no indels introduced into the sequence).

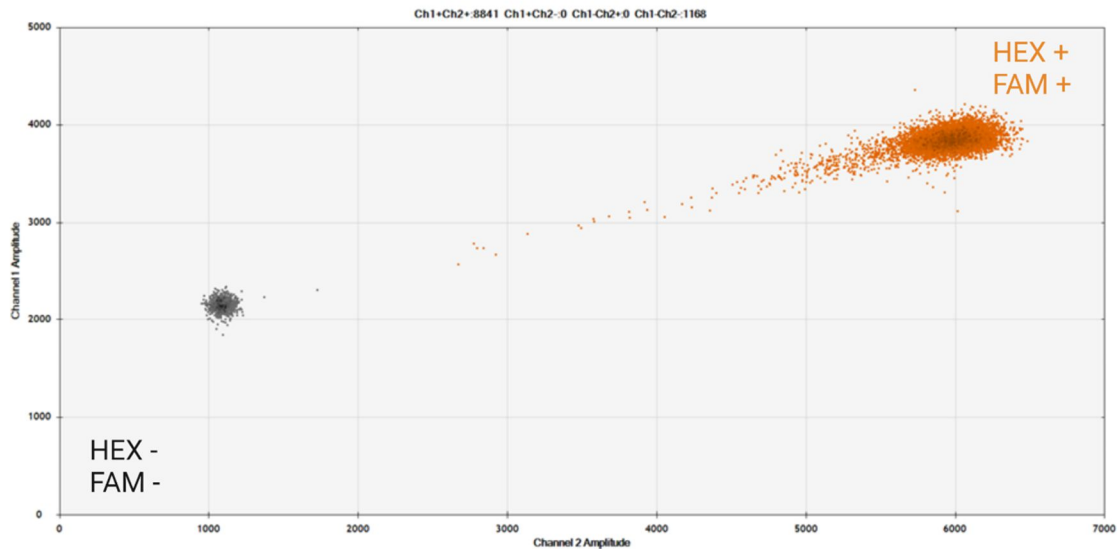


Figure 3.2: NHEJ gating of control PBMCs in a 2D amplitude plot.

The plot shows a 2D Amplitude plot where the amplitude of channel 1 fluorescence (FAM-NHEJ probe) is plotted against amplitude of channel 2 (HEX probe). As earlier described, the grey dots are droplets with no probes attached, and the orange dots are HEX positive (meaning that it has bounded with DNA marker probe), and FAM positive (meaning NHEJ probe was able to bind to the DNA, which again means that there was no indels introduced into the sequence). That in all means that no DNA sequence changes happened here.

To quantify the frequency of HDR events, the HEX+/FAM+ population was analyzed. HEX+/FAM+ indicates that both DNA marker probe and probe-specific sequence from repair template, has successfully incorporated into the genome, meaning the HDR occurred. HEX will bind DNA of the ADA2 locus, while the HDR probe with FAM is specific for binding to introduced changes in the repair template. The cell populations do not bind FAM, but HEX (HEX+/FAM-) will not have the FAM-probe specific sequence incorporated into the DNA.

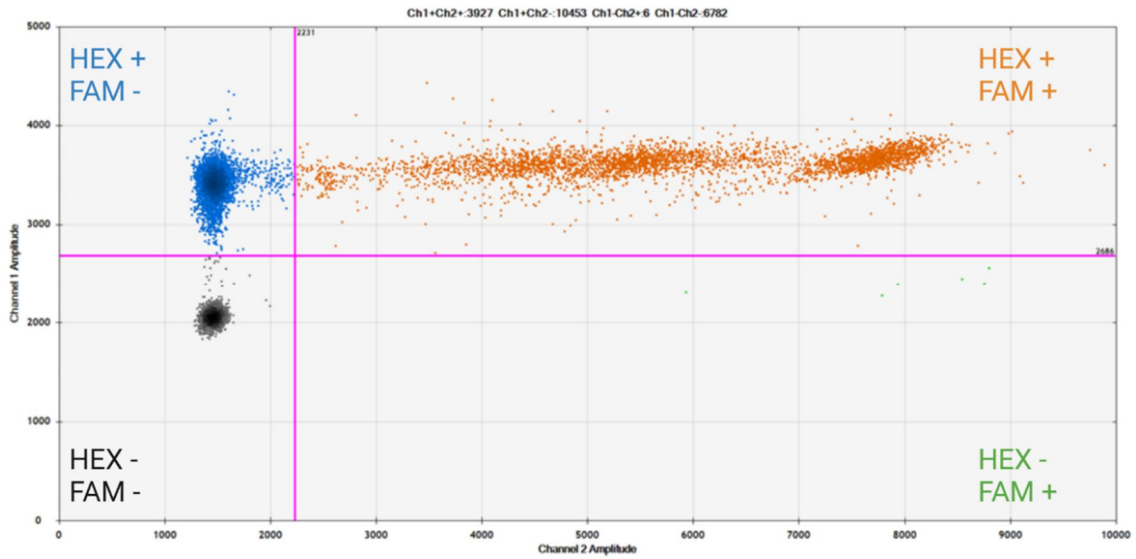


Figure 3.3: HDR gating of *ADA2* knock out PBMCs in a 2D amplitude plot.

It shows a two-dimensional cluster in which channel 1 amplitude fluorescence (HDR probe, FAM) is plotted against channel 2 amplitude (Reference probe, HEX). Population in orange is HEX positive (meaning it has bounded with DNA marker probe), and FAM positive (meaning that probe-specific sequence from repair template has successfully incorporated in the genome, meaning – HDR occurred). Population in blue is HEX positive (meaning it has bounded with DNA marker probe), but FAM negative (meaning that specific sequence from repair template has NOT been incorporated in the genome, meaning – no HDR happened). The population of grey dots are droplets with no probes.

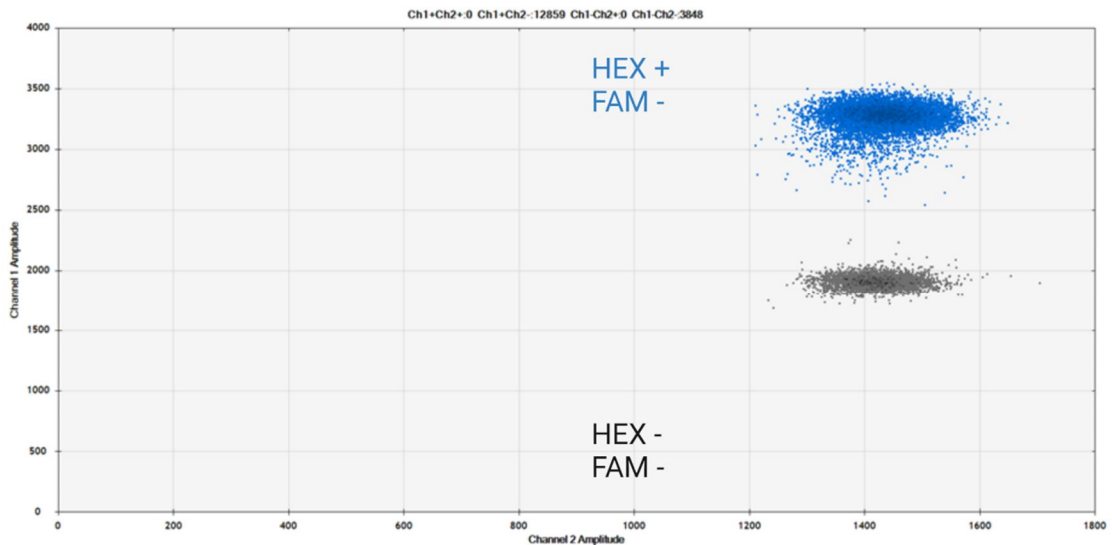


Figure 3.4: represents the negative control well of HDR measurement in a 2D Amplitude plot.

NHEJ gating of control PBMCs. The plot shows a 2D Amplitude plot where the amplitude of channel 1 fluorescence (FAM-*NHEJ* probe) is plotted against amplitude of channel 2 (HEX probe). The grey populations are droplets without probes.

Populations in blue, is HEX positive, meaning that it has bound with the DNA marker probe, but is FAM negative, which means that the specific from repair template has not incorporated into the DNA, meaning no HDR has happened.

The gating for all completed knockout experiments showed population of HEX+/FAM+ for knockout of *ADA2* gene editing with CRISPR/Cas9. The population shows that it was able to bound with the DNA marker probe and that the NHEJ probe was able to bind to the DNA, meaning that there were no indels introduced into the sequence, demonstrating that *ADA2* knockout occurred.

The gating for knock in of R169Q showed population of HEX+/FAM+, meaning that the population had both bounded with DNA marker probe and that the HDR probe-specific sequence from repair template containing the R169Q mutation had successfully incorporated in the genome, and therefore HDR occurred.

The CRISPR/Cas9-mediated electroporation experiments targeting *ADA2* gene, involving knock-out of *ADA2* and knock-in of R169Q mutation in *ADA2*, were successfully performed.

The data obtained from FAM/HEX gating analysis was subsequently exported to Microsoft Excel for calculation of editing efficiencies for NHEJ and HDR-mediated DNA repair mechanisms, pertaining to the *ADA2* gene knock-out and *ADA2* R169Q mutation knock-in experiments. To obtain adequate knock-out efficiency, the KO experiment was done multiple times. Samples shown in pink and blue bars (figure 3.5) were deemed suitable for downstream analysis based on the observed editing efficiency of 22% and 24% from donor 2, and 11% and 10% from donor 1 (figure 3.5). Due to time constraints, the knock-in transfection for the R169Q mutation was conducted only once, with a HDR editing percentage of 27.4% for donor 1 and 14.1% for donor 2. The overall efficiencies for KO and KI is presented in bar charts in figure 3.5.

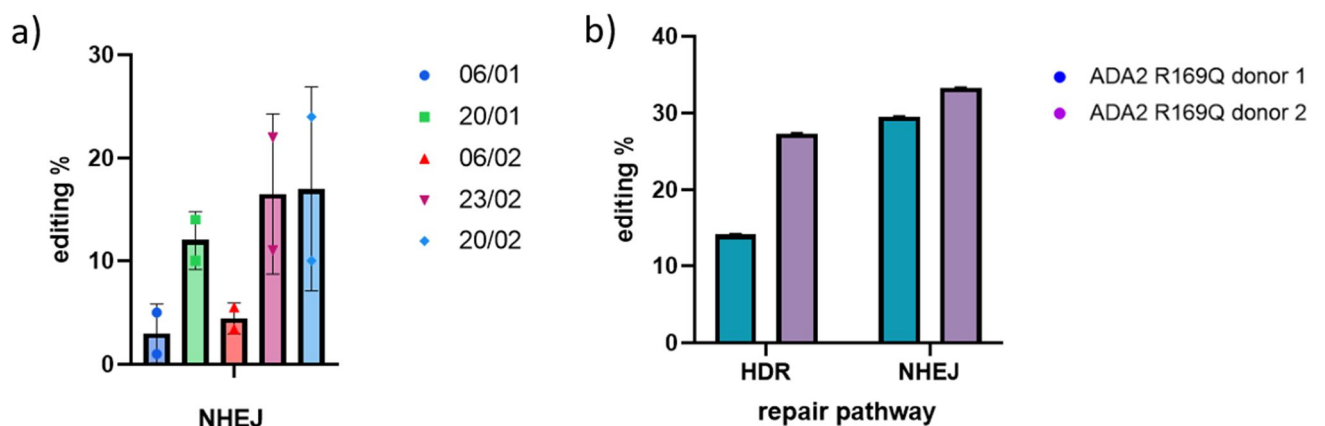


Figure 3.5: editing efficiency of ADA2 knockout and ADA2 R169Q mutation knock in of pbmcs

a) editing efficiency of ADA2 knockout where the bar chart presents the results of a series of experiments aimed at assessing the efficiency of CRISPR/Cas9-mediated gene editing in ADA2 knockout cells done on different timepoints. The x-axis of the figure indicates the date on which the experiments were performed, with y-axis representing efficiency percentage of editing outcome. Each bar represent the mean editing efficiency for both donors used. editing efficiency of ADA2 knockout cells using CRISPR/Cas9 in electroporation on different dates during the project. The editing efficiency was significantly better overtime. b) editing efficiency of the HDR and NHEJ repair pathways of ADA2 R169Q mutation knock-in in two donors. The bar chart presents the editing outcome for both HDR and NHEJ. The x-axis indicates repair pathway, while y-axis represents efficiency percentage of editing outcome.

3.2 Evaluation of ADA2 Gene Knockout and Knock Kn of R169Q Mutation

The samples that had been previously subjected to electroporation and analyzed via ddPCR were subsequently assessed using the Diazyme ADA2 enzyme activity assay to determine their enzymatic activity levels. For ADA2 enzyme activity, the standard curves were successfully made.

The CRISPR/Cas9-edited samples exhibited significantly lower ADA2 enzyme activity compared to the healthy control group, especially for samples of donor 2 [0.23,0.24) vs (0.65,0.72)].

The samples derived from donor 2, which display superior editing efficiencies from ddPCR of 26% and 22% in contrast to donor 1, exhibit significantly diminished ADA2 activity relative to both the control samples and the donor 1 samples characterized by lower editing efficiency of 12% and 11% (figure 3.6). The observed differences between the R169Q knock-in samples and the knock-out samples were not substantial.

Each bar of figure 3.6 show the average of two individual measurements done for validating the results. For the samples of donor 1, the enzyme activity measured for each individual measurements had different activity level for both times, with a difference of 0.34 and 0.55 U/L for ADA2 KO, and 0,36 and 0,65 U/L for ADA2 R169Q KI. There could be various reasons for these differences, which will later be described in the discussion part.

Measurements were done on the medium used for cultivation of the sample cells. Measuring ADA2 activity in the media that cells were cultivated in provides valuable insights into the cellular-environment interactions and helps to gain more comprehensive understanding of

cellular behavior and enzyme activity. However, the Immunocult medium that was used gave unexpected results with wrongly measurements that was not used further in the project. This is further described in the discussion.

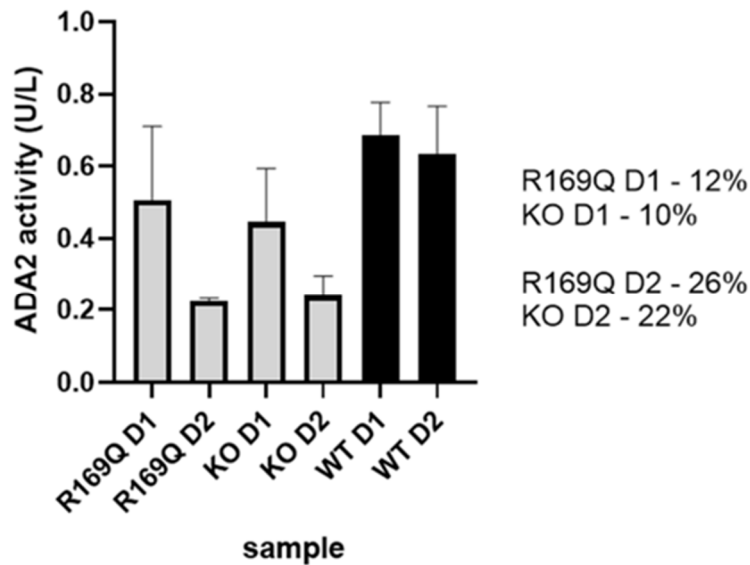


Figure 3.6: Enzymatic ADA2 activity assay in wildtype T cells, R169Q mutants, and ADA2 KO.

Each bar in the graph represents the mean of the ADA2 activity data obtained from each sample, which was validated by performing two independent measurements. The Y-axis indicates the level of ADA2 activity measured in units per liter (U/L) observed in each sample, while the X-axis presents the individual samples being analyzed. Median ADA2 activity is significantly lower in edited samples compared with controls [KO(0.45,0.24), R169Q (0.5, 0.22) vs (0.64,0.6)].

3.3 Evaluation of The Loss of *ADA2* Transcript in *ADA2* Knockout and Knock In of R169Q Mutation

The fold change indicates whether a gene is up-regulated or down-regulated. The fold change in the samples with *ADA2* knocked out shows a fold change of 0.655 and 0.48, meaning a 65.5% and 48% gene expression relative to the control condition, which has all been normalized to the SS18 housekeeping gene.

Donor 1 with *ADA2* mutation R169Q knocked in, have a fold change of 1.049, meaning that there is 100% as much gene expression in the sample as in the control condition, indicating that there is no change between the mutated sample and the control. Donor 2 with *ADA2* mutation R169Q knocked in, have 83% gene expression relative to the control, indicating down-regulation (figure 3.7).

The results of gene expression in the samples are presented as fold-change bar charts graphing the control condition equal to 1.

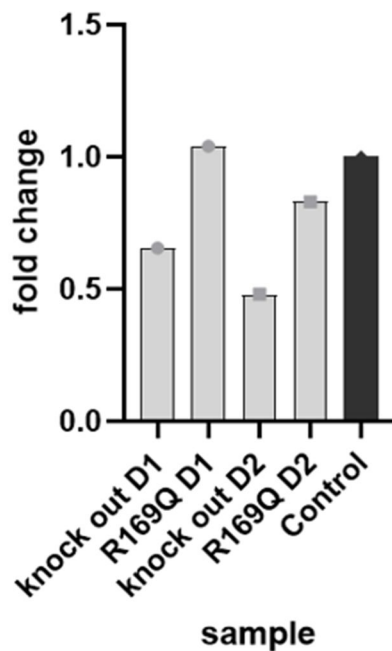


Figure 3.7: evaluation of downregulated ADA2 transcription.

Y-axis indicates the fold change of ADA2 protein, while X-axis presents the donor samples (grey) and control (black). Donor 1 KO (= 0.655) and donor KO 2 (= 0.48), and donor 1 KI R169Q (= 1.049) and donor 2 KI R169Q (= 0.83) edited samples compared to control value (=1). Figure made in GraphPad Prism 9 (Dotmatics).

3.4 Effect of ADA2 Knockout and R169Q Mutation Knock in on T-cells

To study the impact of ADA2 R169Q mutations and downregulation on T-cell functioning, assays were conducted to assess T-cell proliferation and activation using flow cytometry.

By combining the FSC and SSC light signals earlier described into a graph, a graphical representation known as dot plots is formed. Each individual dot on these graphs represents an individual cell.

A representative gating strategy was used based on gates set using FMO and compensation controls. SSC versus FSC was used to gate the overall cell population of lymphocytes. Single cells were then gated using the FSC-A versus FSC-H plot, before gating the live cells using a sample with 50% live, 50% dead FVD660 stained cells, to distinguish the live cell population

from the dead cells (figure 3.10). The remaining plots are plots (figure 3.11-3.13) of the respective markers. For T-cell activation: CD3, CD4, CD8, CD25 and CD69. For T-cell proliferation: CD3, CD4 and CD8.

Before compensating data in FlowJo, parameters which require compensation were scaled correctly.

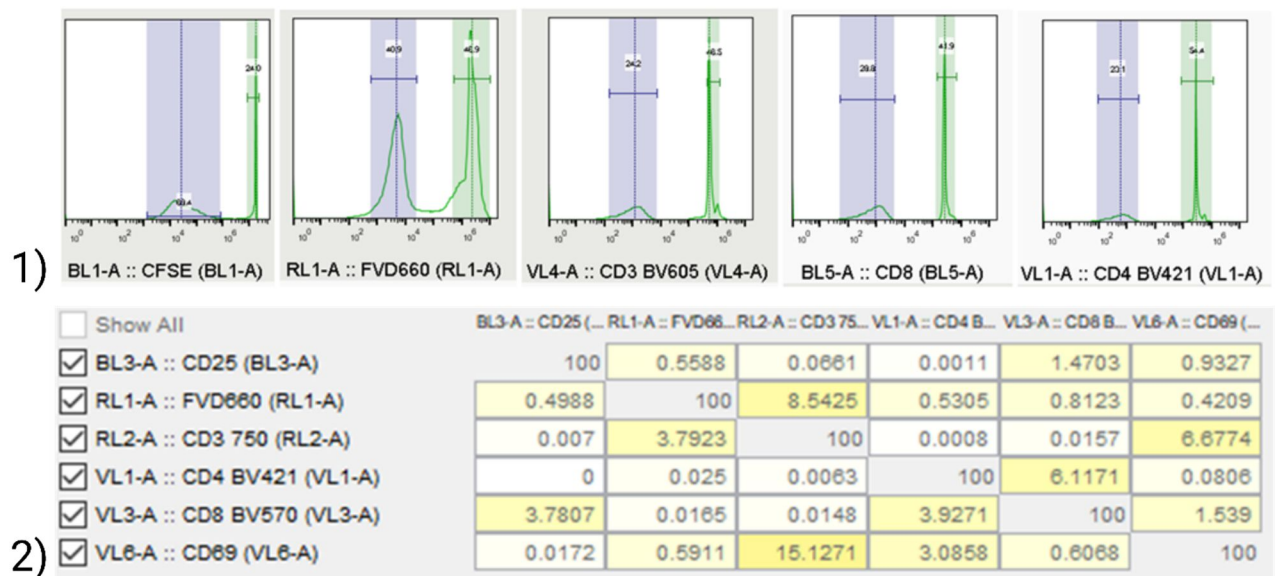


Figure 3.8: Compensation matrix from FlowJo

1) Compensation gating of CFSE, FVD660, CD3, CD4 and CD8. The blue gate shows the negative population, and the green gate shows the positive population.

2) The table shows the compensation matrix generated after setting up the compensation. The table shows the spillover of the various antibodies into the various channels. It was acquired by FlowJo. The lower the values are, the better the analysis by using compensation is. The compensation was made using compensation beads.

The data underwent a gating procedure to isolate the cells of interest. Figure 3.9 illustrates the gating strategy that was employed during this process for identifying and selecting the live cell population. Further, gating was performed based on the presence of surface antigens that are specific to T-cells. This additional gating step allowed for the isolation of the specific T-cell subtypes that were of interest in the study and are shown in figure 3.11-3.13.

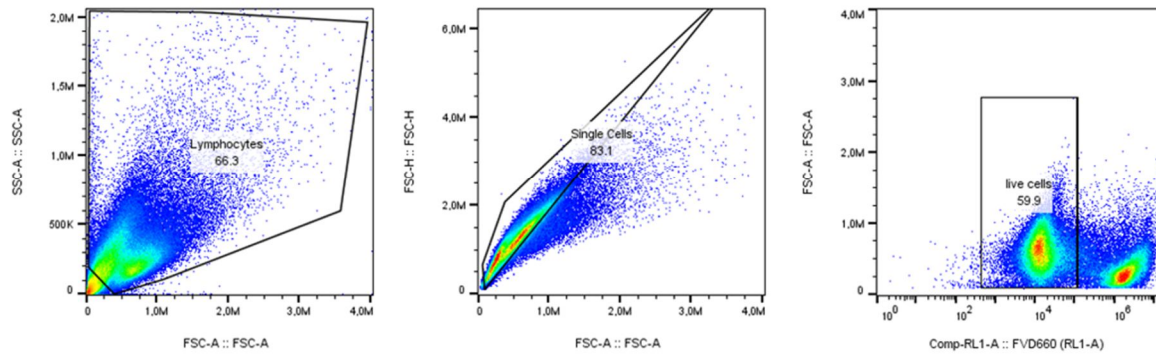


Figure 3.9: gating strategy of T-cells using FlowJo.

The T-cells were gated in FlowJo to get the live cell population. The gating procedure consisted of sequentially identifying lymphocytes, single cells, and live cell populations.

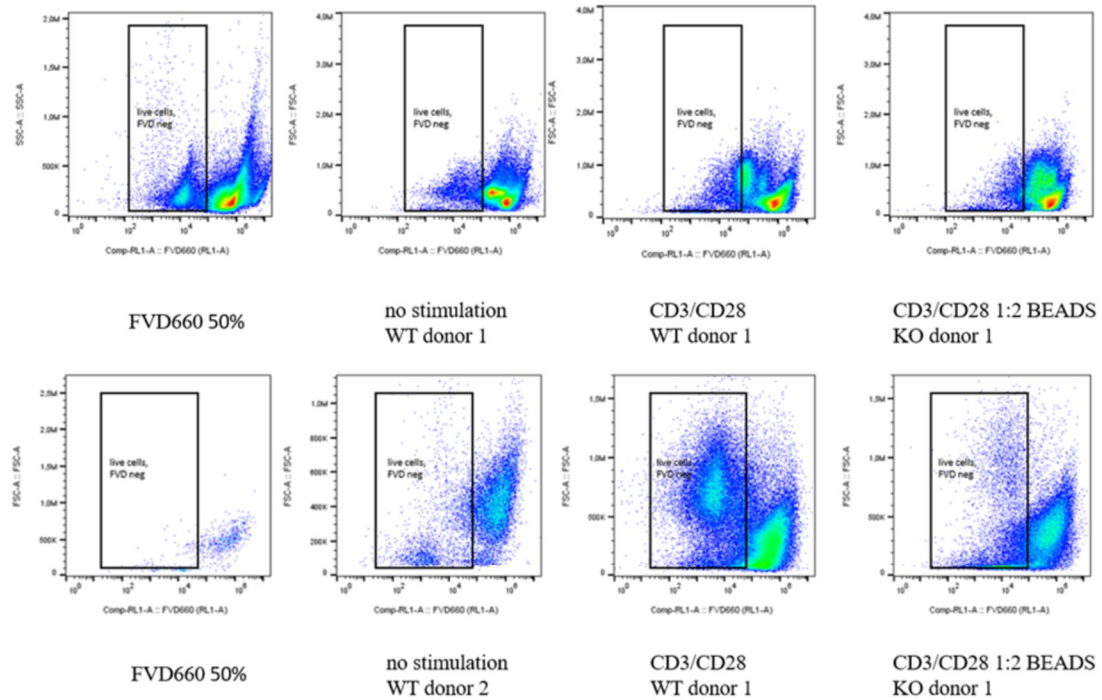
3.5 The Effect of Long Culturing vs Short Culturing on CRISPR/Cas9 Edited PBMCs for T-cell Activation

Assay

The T-cell functions assays were done by studying T-cell activation and proliferation of short cultivated WT T-cells and of long cultivated T-cells of three different types of T-cells: *ADA2* KO and R169Q KI edited T-cells, and WT T-cells. The cells undergoing short cultivation were cultivated for 48 h for activation assay and 6 days for proliferation assay. For the long cultivation, cells were in culture for 12 days for activation assay and 16 days for proliferation assay.

The use of FVD660 gating for flow cytometric analysis revealed a high frequency of cell death in the samples cultured for 14 days following electroporation (EP) as illustrated in figure 3.10. Additionally, the cell yield was observed to vary significantly between individual samples, although the quantity of cells seeded were consistent across all samples with the concentration of 100 μ l/l in each well. In comparison, samples cultured for only one day exhibited a markedly higher cell viability and yield (figure 3.10). The findings suggest that prolonged culturing post-EP may have a disadvantageous impact on cell viability, and the effect may be variable across different samples. It is important to consider these factors when interpreting the results obtained from samples subjected to prolonged culturing times following EP.

long cultivated cells



short cultivated cells

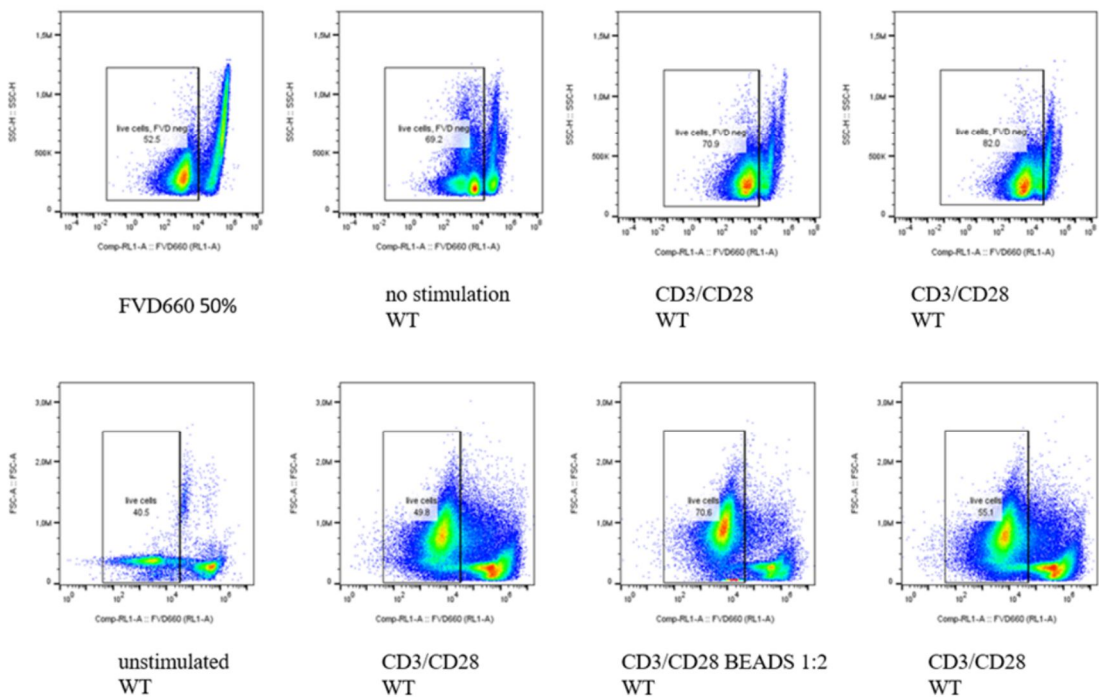


Figure 3.10: gating of live cells/dead cells with FVD660 dye.

The gatings are done with FSC-A scattering on the Y-axis and the compensation of the stimulation tested on the x-axis. The set of experiments are parted into rows. The first two rows includes gatings of the flow experiments with long culturing and the last two rows of cells with short culturing. Where the cells stained with CFSE for proliferation is at the 1. and 3. row, and cells for activation assay are in the 2. and 4. row. As seen in the figure the quantity of dead cells compared to live cells is significant, with in general low and varied quantity of cells between the samples. The black squares represent the live cell population. In these first two rows, FMO 50% FVD660, non-stimulated samples of WT, KO cells with bead stimulation and CD3/CD28 stimulation of WT cells are included. Selected data are used here. The rest of data is not shown. For row 3. And

4., gatings of FMO 50% FVD660, unstimulated, CD3/CD28 and beads stimulated WT cells are shown. The black squares represent the population of live cells and the numbers in the squares, presents the percentage of live cells. Selected data are used here. The rest of data is not shown.

As seen for the gating of CD3+, CD4+ and CD8+ for long cultured cells, the antibodies did not bind to any or just a few number of cells (figure 3.11-3.13). Especially for the long-cultured T-cells stained with CFSE for proliferation assay, the population displayed a notably diminished cell quantity. However, the abundance of cells exhibited significant variation across all different samples and was generally low. Also, the FMOs for CD4 and CD8 did not work for long cultivated cells. The short-cultivated cells were placed together with the long-cultivated cells in these figures, to show how gating the T-cell subsets should look like.

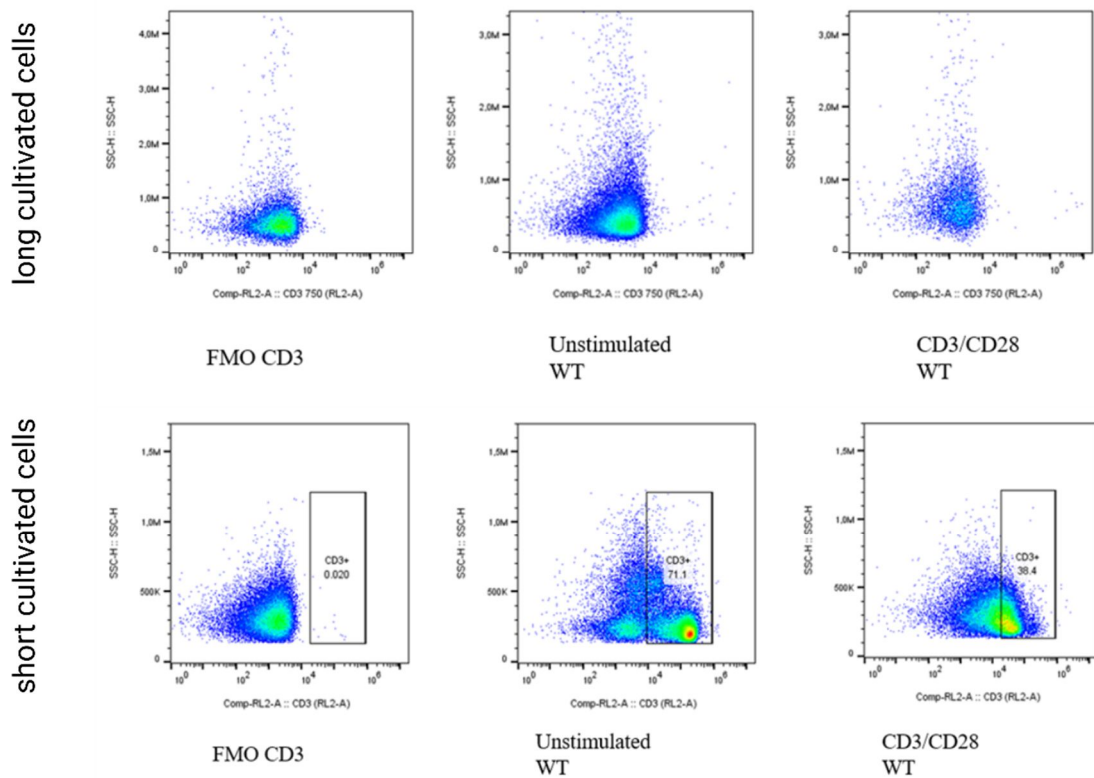
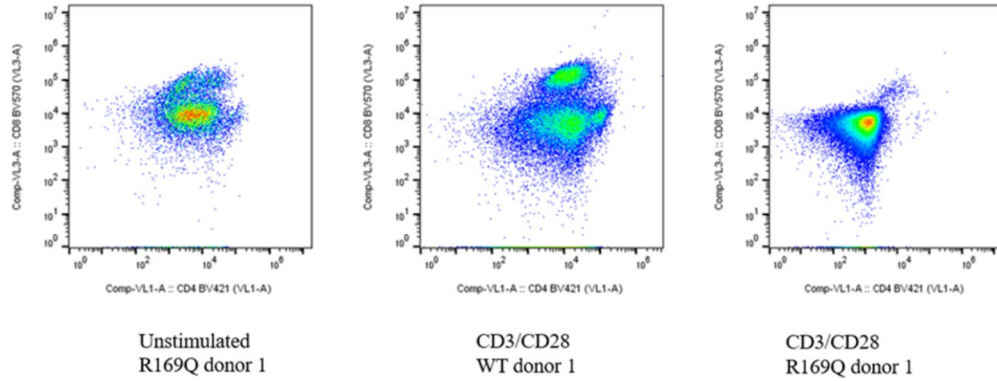


Figure 3.11: CD3+ gating of long cultured and short cultured of activation assay.

The gatings are done with FSC-A scattering on the Y-axis and the compensation of the stimulation tested on the x-axis. These gatings compare FMO of CD3+, unstimulated cells and cells stimulated with CD3/CD28. The long-cultured cells (first row) show no results for CD3+, compared to the short-cultured cells (second row) with a percentage of 71,1 and 38,4 of CD3+subset. Selected data are used here. The rest of data is not shown.

long cultivated cells



short cultivated cells

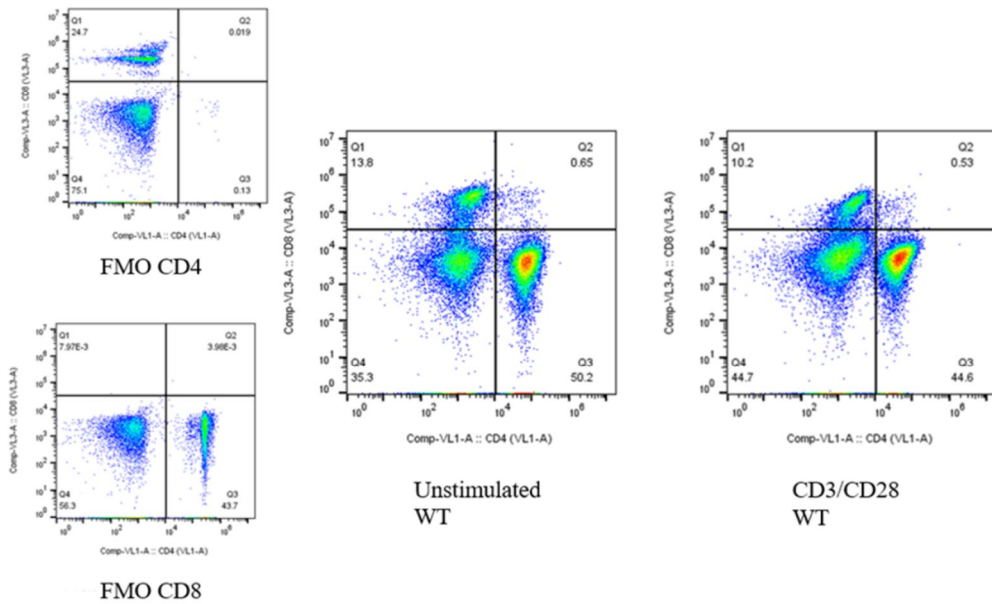


Figure 3.12: CD4+ and CD8+ gating of long cultured (first row) and short cultured (second row) of activation assay. The gateings are done with compensation of CD8 on the Y-axis and the compensation of CD4 on the x-axis. These gateings compare FMO of CD4 and CD8, unstimulated cells and cells stimulated with CD3/CD28. The long-cultured cells show results that are too dense to be separated into subgroups compared to the short-cultured cells with a correct FMOs and subgroups of 50.2% and 44.6% for CD4. Selected data are used here. The rest of data is not shown.

The antibodies, except for the CD25 and CD69 used in the T-cell activation assay, bound to the cell surface of short-cultivated samples. The CD25 and CD69 antibodies did not bound for the long-cultivated cells either as seen in figure 3.13.

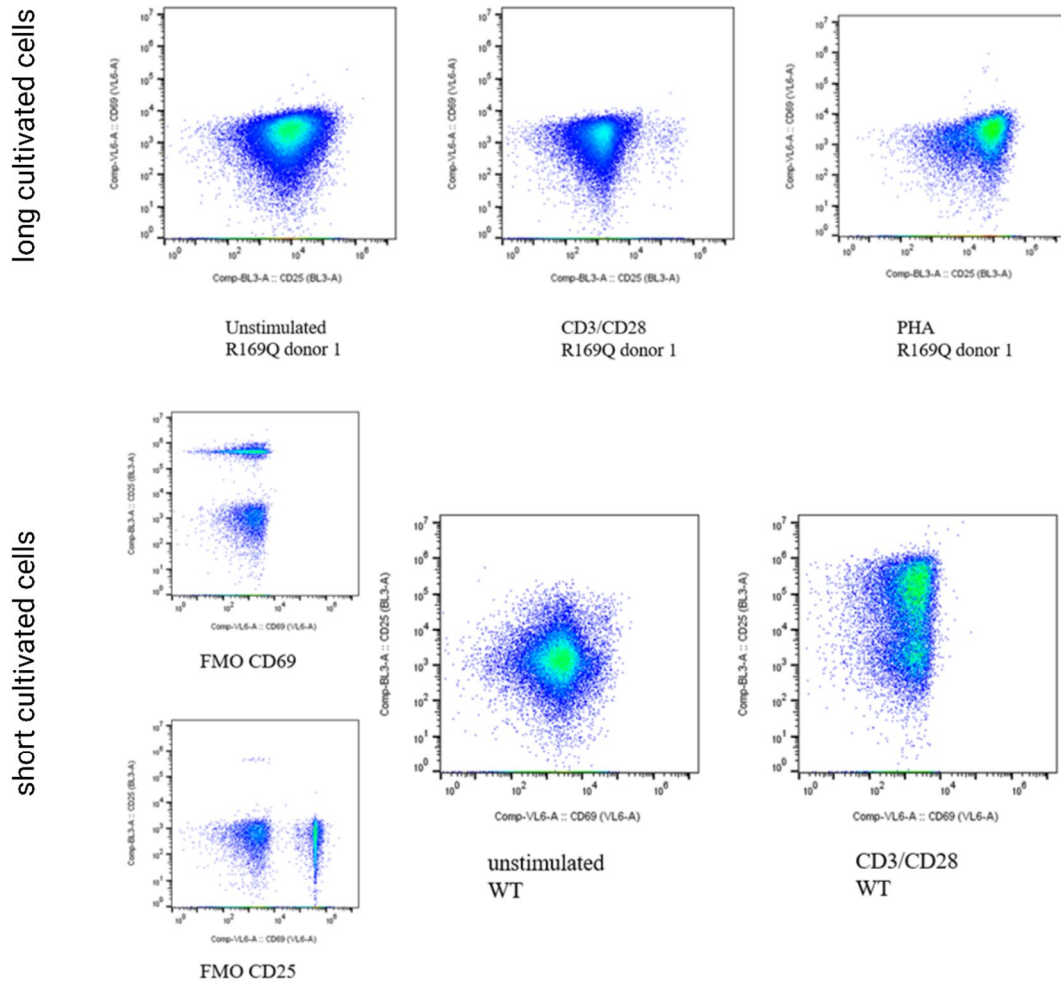


Figure 3.13: CD25 and CD69 gating of long cultured and short cultured of activation assay.

The gateings are done with compensation of CD25 on the Y-axis and the compensation of CD69 on the x-axis. These gateings compare FMO of CD25 and CD69, unstimulated cells and cells stimulated with CD3/CD28, including one PHA stimulated well of the long-cultivated cells. For both the long-cultured cells (first row) and short-cultured cells (second row), results that are too merged to be separated into subgroups and did not work for stimulation of neither experiments. Selected data are used here. The rest of data is not shown.

The percentage of the populations gated of CD3+, CD4+ and CD8+ in the short-cultivated cells from the proliferation experiment were further visualized in figure 3.14. The various samples of T-cells are represented using distinct color codes.

The samples not stained with CFSE showed lower much lower percentage of CD8+ cells compared to percentages of both CD3+ and CD4+. With the overall highest population of CD3+ cells for all samples.

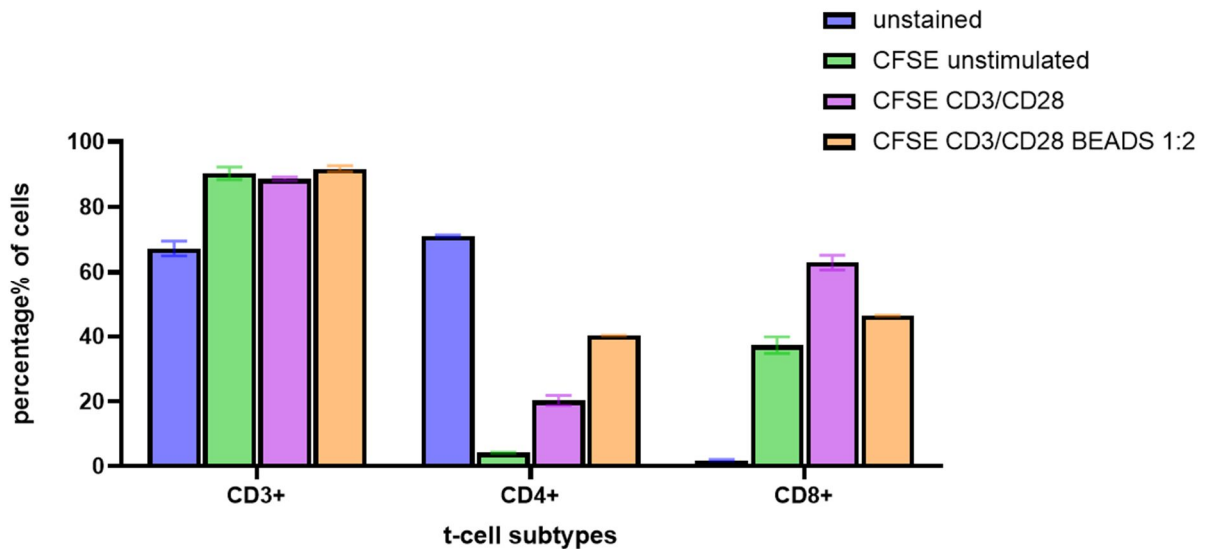


Figure 3.14: bar chart showing the percentage of different cell subsets gated in both unstained and T-cells stained with CFSE, stimulated with CD3/CD28 antibodies and CD3/CD28 beads in color codes.

Y-axis represents the percentage of cells in the subsets, and the x-axis represents the t-cell subsets. This chart represents the cells of short cultivation period in the proliferation assay.

3.6 Effect of Long Culturing vs Short Culturing on CRISPR/Cas9 Edited PBMCs for T-cell Proliferation Assays using CFSE Staining

The platform proliferation modeling in FlowJo was used for tracking the number of divisions that a CFSE-labeled cell goes through. When tracking the quantity of cell divisions in response to a stimulus, it is possible to determine whether the cells exhibit a proliferative response to the given stimulus.

For the short-cultivated cells only including the WT T-cells, the degree of proliferation is illustrated in figure 3.15. The percentage of divided cells were the highest for CD8+ cells and overall, for the cells stimulated with CD3/CD28 antibodies. For the cells stimulated with CD3/CD28 Dynabeads, the proliferation is quite similar to the cells stimulated with CD3/CD28 antibodies. For CD8+ cells, both division index and percentage divided is low, indicating that there was a small population of CD8+ positive cells compared to CD3+ and CD4+.

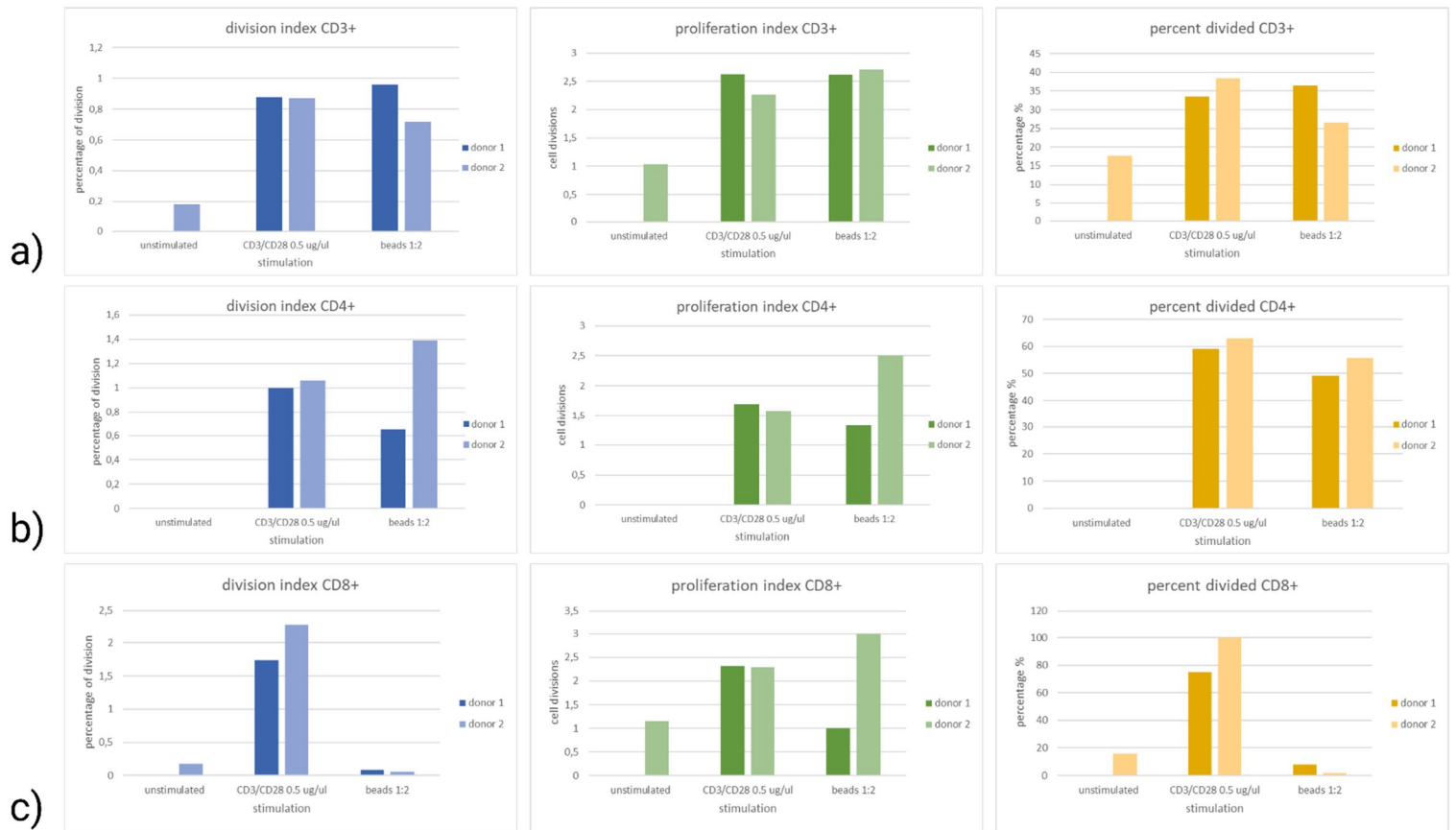


Figure 3.15: bar charts representing the division index (blue), proliferation index (green) and percent divided (yellow) and the subset populations of a) CD3+, b) CD4+ and c) CD8+.

The charts show unstimulated cells, cells stimulated with CD3/CD28 antibodies and CD3/CD28 beads. The cells in this analysis are short cultivated WT T-cells from two different donors. Y-axis represents the percentage of divided cells, and the x-axis represents type of stimulations.

For the long-cultured cells, the CFSE stain did not work, as seen in figure 3.16. The cells of long cultivation did not get the nice and distinct peaks from CFSE staining as for the short-cultivated cells, as seen in the figure.

A part of the project was to compare and evaluate proliferation rates among the different experimental groups: ADA2 KO, ADA2 R169Q KI and WT T-cells, however because of CFSE not staining the long-cultivated cells, this analysis was not possible to take further.

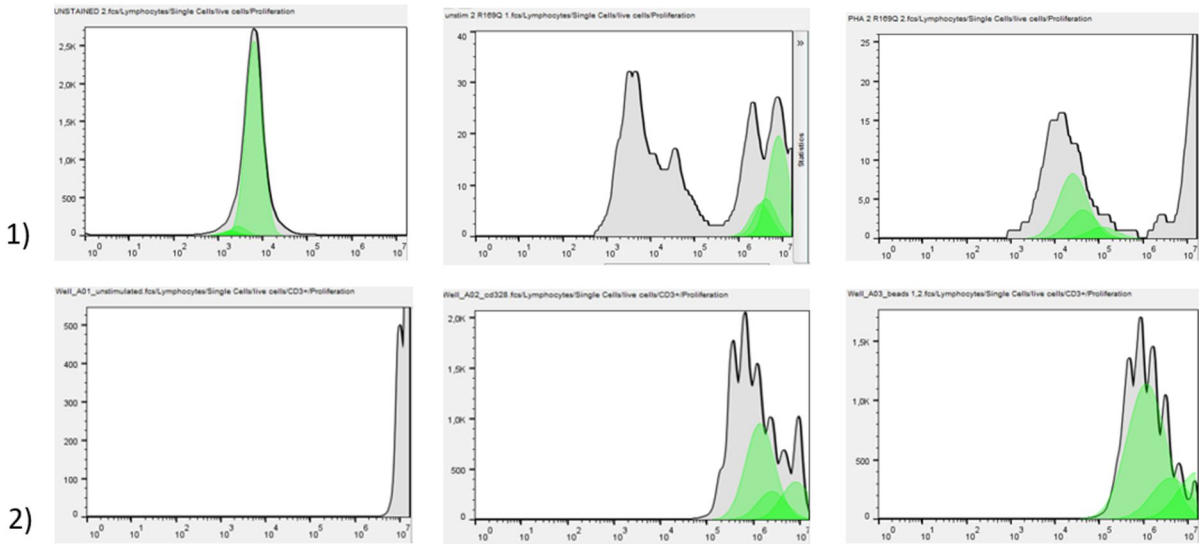


Figure 3.16: proliferation modeling of T-cells comparing short and long-stimulated cells.

1) represent the long-cultivated cells including an unstained and two R169Q knock in samples, where the middle one shows the proliferation of unstimulated sample and the one to the right show a PHA stimulated sample. 2) represent short-cultivated cells including an unstimulated sample and two stimulated WT samples stimulated with CD3/CD28 antibodies in the middle and the one to the right stimulated with CD3/CD28 beads.

4 Discussion

By performing a variety of different experiments, some important insights into the conditions of a T-cell expansion culture and of the mechanism of the DADA2 disease have been gained.

4.1 *ADA2* Editing in T-cells

CRISPR/Cas9 technology has emerged as a powerful tool for genome editing due to its ability to induce site-specific double-strand breaks (DSBs) in the genome. Subsequent repair of these breaks by the cellular machinery allows for the introduction of desired genetic modifications (Adli, 2018). Electroporation (EP) is a widely used method for introducing foreign DNA into target cells involving the application of brief electrical pulses to create temporary pores in the cell membrane, to allow the uptake of exogenous molecules. EP was chosen as the delivery mechanism for the CRISPR/Cas9 components into the target cells. This approach offers various advantages, including efficient delivery of the gene editing reagents, applicability to a wide range of cell types, and compatibility with high-throughput experimentation (Yarmush et al., 2014).

Despite the theoretical promise of this combined approach, practical difficulties were encountered during the experimental phase. Significant challenges were encountered in achieving a desirable level of editing efficiency utilizing the CRISPR/Cas9 system combined with electroporation. The efficiency of the editing process, as measured by the rate of successful genome alterations, was considerably low. Only the last round of electroporation with transfection efficiencies of 22% and 26% for KO and KI, was used further.

There are various factors that can influence editing efficiency with electroporation of CRISPR/Cas9, including purity of components used, cell type, donor variety, optimization and accuracy or technical errors (Lino et al., 2018).

Using electroporation for editing PBMCs, the transfection efficiency can vary depending on several factors. It is important to use high-quality PBMCs and optimization of electroporation parameters may be added to achieve the highest editing efficiency while minimizing cell damage.

The PBMCs used in this project were of high quality, being obtained from freshly collected buffy coats and protocols employed in this project underwent prior optimization specifically

tailored to PBMC cells to enhance their editing efficiency and should therefore not have had a huge impact for the low editing outcomes.

There are donor-to-donor variability in editing efficiency when working with PBMCs cells, as seen in the result variety between donor 1 and 2 where the editing efficiency has a difference of 10% between the donors. Some people may have highly effective repair mechanisms, that leads to lower editing efficiency and vice versa, due to the immune system being highly variable between individuals (Brodin & Davis, 2017). Specific factors including age, health status and medical history may also impact the variability between donors. The health status may affect the quality of PBMCs which then again may impact the cells' response to editing.

Individual genomes may affect efficiency of the editing, and variables are therefore important to consider when comparing and interpreting transfection efficiencies across various individuals (Boston Children's Hospital, 2017). A consideration would be to perform the experiment with multiple donors to account for the variation. It is essential to ensure that the observed editing efficiencies are both robust and representative to guarantee their accuracy and validity. Due to time constraints the experiments were done with 2 donors, however testing on multiple donors should be considered in future work.

While electroporation is a widely used method for gene editing, high editing efficiencies are not always achieved, because of the heterogeneity and specific characteristics mentioned above. Researchers are continually studying and developing alternative methods for delivery and techniques for increasing the editing efficiency in PBMCs (Abdelnour et al., 2021).

Technical errors, including improper handling of cells may result in reduced efficiency of editing, making the cells less responsive to editing components. Unfortunately, due to limitations in time, it was not possible to improve the editing efficiency of the cells. However, these strategies could be taken into use if time allowed.

4.2 Downregulation of *ADA2* Gene Expression Gave Lower Protein Activity

The results from ADA2 enzyme activity test show that there are noteworthy differences between the ADA2 activity in the mutation sample and KO sample compared to the WT samples (figure 3.6). The results indicates that a knock-out of *ADA2* has happened in the KO

sample, because lower amount of the gene will result in lower activity of it. As seen in the figure (figure 3.6), the R169 knock-in and KO samples have quite similar amounts of activity. A previous study done on nine patients with *ADA2* deficiency due to R169Q mutations, found that *ADA2* enzyme activity was significantly lower in the patients compared to the control groups (Van Montfrans et al., 2016), which makes this knock-in of R169Q samples valid.

As seen in the figure (figure 3.6), the observed *ADA2* activity exhibits variability between the two donor samples, which is due to the editing efficiency differences between the donors as described in section 4.1. However, the enzyme activity varies between the control samples of the donors also. The amount of *ADA2* activity can vary among individuals, and be influenced by various factors, as described in an article where they observed that *ADA2* activity decreases with age (Bowers et al., 2020). The observed differences in gene activity between the two donors is likely attributable to the complex interaction of genetic, physiological, and environmental factors influencing the enzymatic function of *ADA2*. These interactions can lead to variations in the gene expression and activity of *ADA2*.

Even though these results are promising, further research and studies are needed to fully elucidate the relation between the R169Q mutation and *ADA2* enzyme activity. Using multiple donors with a minimum of 10-20 per group, to also observe that the differences between samples are statistically meaningful.

Another important aspect of the resulting measurements of enzyme activity is that the measurements done on the lower edited 2. donor, shows a variability between the first and second measurement. This means that the editing needs to be of a higher percentage to be trustworthy, like the donor 1 samples where the difference between the two measurements are low. There could be various reasons for this phenomenon, including genetic variation in the population leading to differences in the expression or activity of *ADA2*, resulting in varying measurements.

Regarding the result of the R169Q variant with a fold change of 0.83 and the knockout of *ADA2* with a fold change of 0.48 present some insights into the functional consequences of genetic alterations were gained.

The R169Q donor 2 variant suggests that there is a potential decrease in gene expression compared to the control group of non-edited cells (figure 3.6). In addition, the knock-out showed a great decrease in expressing the *ADA2* gene, with a fold change of 0.48, meaning 48% expression of the gene.

The fold changes in the samples showed greater editing efficiency using qPCR than ddPCR. ddPCR is more sensitive and precise than qPCR. A reason for ddPCR having lower editing efficiency could therefore be due to detecting low frequency edited alleles that qPCR may miss (Taylor et al., 2017). As a result, the editing efficiency done by ddPCR might give lower editing outcomes due to the ability to detect rare events.

The correlation between the downregulation of gene expression in relation to *ADA2* activity suggests that a decreased activity of *ADA2* may lead to reduction of gene expression levels. The outcomes from the measurements done on *ADA2* activity and of gene expression with qPCR, and the theoretical expectations is conspicuously strong, indicating a notable correspondence.

Comparing the *ADA2* activity measurements of *ADA2* KO and KI of R169Q (figure 3.6) with the gene expressions (figure 3.7), the samples of donor 2 that have been previously explained as the donor with better editing efficiency had the lowest gene activity measured of 0.24 U/L for R169Q and 0.22 U/L for KO. The same samples had a reduced gene expression with the lowest results of 0.48 for KO and 0.83 for R169Q. This present that there was association between downregulation of gene expression giving lower *ADA2* activity.

Although certain positive outcomes were accomplished, the experimental studies encountered some limitations. One limitation was the sample size utilized for the study. The samples used were relatively small, which restricted the generalizability of the study. Taking use of a wider set of samples including both edited and control samples from multiple donors would give a wider representative analysis and reducing the potential of errors, by the possibility of using statistical tests for significance.

Another consideration is that the variability in *ADA2* activity within the populations, that are being measured including factors like genetic variations and medical history may affect the reliability and accuracy of the results.

It is also possible to test samples of media that were described in the method part. *ADA2* is known to be secreted by cells into the extracellular environment, compared to *ADAI* (Anton V. Zavialov et al., 2010) and therefore by testing samples containing medium that the cell samples previously have been cultured in, evaluating of the release and secretion of *ADA2* by the cells can be done. Which can help in understanding the regulatory mechanisms and dynamics of *ADA2* secretion. As mentioned in the results, the Immunocult disrupted the

measurements giving false results compared to using the RPMI media. To use Immunocult media in future activity tests, optimization of the protocol is needed.

The observations done raise questions about the impact of the R169Q variant on the underlying biological processes, indicating that a regulatory effect on transcriptional activity or post-transcriptional processes may contribute to the observed fold change. Further studies into the specific mechanisms underlying R169Q are necessary for providing insights into its functional and potential association with phenotypic outcomes.

4.3 Variability in T-Cell Activation and Proliferation Assays with Long-Cultured Edited T-Cells"

In T-cell activation assays, R169Q mutated samples and KO samples were studied using WT samples as controls as well as including FVD660 viability dye for selectively enter cells with compromised plasma membrane integrity, such as dead or non-viable cells for distinguishing live cells from dead. FMOs as earlier described was used for validating compensations.

The cells undergoing long cultivation were as described in section 2.9.4, cultivated for 12-16 days. Long culturing of T-cells before a flow cytometry assay can be beneficial for several reasons, including that T-cells require a certain period in culture to be able to differentiate into specific T-cell subsets or to become fully activated. As described in this article, T-cells need around 7-15 days after stimulation (Pennock et al., 2013). When extending time in culture, it allows for the development of desired functional properties and phenotypes, which again will enhance the ability to investigate specific T-cell subsets or functional states when doing the flow cytometry analysis.

The stimulation and viability outcomes of short culturing was significantly better in T-cells that went through a short cultivation period. As seen in figure 3.10 from the gating of live cells with the use of FVD660, both the short-cultivated cells for activation assay and cells stained with CFSE for proliferation assay have a viability percentage of 40-82%, compared to the long-cultivated cells with a viability going from none to 1/5 of the cells being alive.

Binding of antibody to surface for the short-cultivated cells, whereas previously mentioned none of the cells were edited, FMOs were working for all antibodies. The antibodies bound to the surface for all antibodies except for the CD25⁺ and CD69⁺ antibodies used for the T-cell

activation assay. CD25⁺ and CD69⁺ are typically associated with T-cell activation (Borges et al., 2007), (Reddy et al., 2004). If the expression of these antibodies are low or absent on the cell surface, the cells would be in a resting or non-activated state, indicating that these cells would not have been activated during the experiments.

As seen for the gating of CD3⁺, CD4⁺ and CD8⁺ for long cultured cells, the antibodies did not bind to any or just an insignificant low number of cells. Especially for the long-cultured T-cells stained with CFSE, the population displayed a notably diminished cell quantity. However, the abundance of cells exhibited significant variation across all different samples and was generally low. Also, the FMOs for CD4⁺ and CD8⁺ did not work for long cultivated cells.

The low abundance of antibodies to T-cell surfaces have been mentioned to be insufficient antibody concentrations, where the concentration is too low and therefore may not provide enough binding sites to effectively target and bind to the surface markers of the T-cells (Collino et al., 2007). For non-edited T-cells the antibody concentrations have earlier been optimized, however an optimized concentration quantity should be considered for edited T-cells.

Another reasoning for both high quantity of cell death and antibodies not binding to cell surfaces is the long cultivation period, where the cells repeatedly have been experiencing stimulation with IL-2 and one time with CD28/CD3 when first cultivated, which may have led to the cells being too exhausted for another stimulation.

The cell may also have experienced a large amount of stress during processing, in the mechanical and enzymatic procedures involved in the preparation of cells in flow cytometry assays, including the steps cell isolation, washing, and staining, which can induce stress and potentially cell death. The process of editing cells through CRISPR can render the cells more prone to vulnerabilities and subsequent procedures involving washing steps and exposure to toxic EP buffer can exacerbate cellular fragility.

When analyzing the percentage of the populations gated of CD3⁺, CD4⁺ and CD8⁺ in the short-cultivated cells, CD3⁺ had an overall high population rate through all samples as seen in figure 3.14.

For the proliferation assay observing the cells that went through the short cultivation, CFSE staining was successful, however for the longer cultivation the staining did not work.

There is a difference in transfection efficiency between the two donors, especially between the samples stimulated with the Dynabeads. Every individual person have, as described in section 4.1, a unique genotype that influences their immune response, making genetic variation contribute to differences between donors in terms of T-cell proliferation.

For the analysis of longer cultivated cells (section 3.5), the same principles as mentioned for high quantity of cell death and antibodies not binding to cell surfaces in the activation assay applies, including the overstimulation and vulnerability of editing the cells.

The effect of long culturing in rich media, the overstimulation and editing itself is possible reasons for CFSE not staining the cells. CFSE dye was at a final concentration of 5 μM , however, the optimum concentration should be determined for each batch prepared as explained in a previous study (Quah & Parish, 2010) and may have been too high concentrated for these vulnerable cells.

Another outcome of bad CFSE proliferation modeling is inconsistent dilution pattern of CFSE. The intensity of CFSE fluorescence was expected to decrease with every cell division, to indicate successful proliferation. However, if CFSE labeling is not uniform across the cells in the sample or if there are variations in CFSE uptake or retention, it can lead to irregular dilution pattern, as seen in figure 3.16.

In addition, it is worth noting that the T-cells for long-term cultivation were cultured in Immunocult media, while the T-cells for short-term cultivation were cultured in RPMI media. This disparity in the culture conditions, including variations in the composition of the media and the presence of specific growth factors or supplements, could potentially contribute to differences in T-cell proliferation observed between the two groups. The specific constituents of Immunocult media and RPMI media may influence the viability, activation, and proliferation of T-cells, thus influencing the observed variations in T-cell proliferation between the long-cultivated and short-cultivated groups. The immunocult media have been showing robust T-cell expansion and yield a high fold expansion (MacPherson et al., 2022), making the cells grow at a much faster rate, which can have caused the cells to already have gone through the proliferates steps. Proliferation may have occurred on different timepoints for each sample also, due to the differences in editing efficiency throughout the populations.

In this study, issues were encountered related to clogging of the instrument's fluidic pathway that becomes obstructed and an issue were the system failed to properly engage with the designated wells. After a run, some of the wells were not emptied. These issues mentioned that were faced during the latest flow run, could lead to compromised fluidic flow, disrupted sample aspiration, and making the data unreliable. These technical challenges raised some concerns about the accuracy and reproducibility of the data obtained and is another proposition for the unexpected results gained in the flow cytometry assays for long cultivation samples.

For future studies, a wider set of samples including both edited and control samples from multiple donors, can help to further understand the underlying factors contributing to the observed differences in T-cell proliferation.

Ultimately, optimizing the protocol for edited cells and for usage of the Immunocult media is needed, to ensure that the experimental conditions are appropriate for the specific edited T-cell population, including the antibody concentration, buffer composition and incubation time.

4.4 Concluding remarks and future perspectives

The aim of this study was to study the effect of knock out of *ADA2* and knock in of *ADA2* R169Q mutation on the enzyme activity and expression of the *ADA2* gene. And further study the impact of *ADA2* downregulation on T-cell functioning.

The *ADA2* enzyme activity of the KO cells and cells mutated with R169Q revealed lower *ADA2* activity compared to control samples, including downregulation of the *ADA2* gene.

Because of the negative outcomes of stimulation and viability of the long-cultivated edited cells, it was not possible to investigate the functionality of T-cells using these edited cells. Optimizing the protocol for edited cells and Immunocult media is needed for future studies.

5 Appendix I

Includes kits, reagents, equipment, software, and instruments applied in this thesis.

Table 1 Reagents, buffers, mediums, and kits used for this study, with the corresponding distributor, catalog number and assays of usage.

Name	Distributor	Product/catalog number	Usage
Gibco™ RPMI 1640 Medium, GlutaMAX™ Supplement	Fisher Scientific (Leicestershire, UK)	# 12027599	Cell culture
Gibco™ Fetal Bovine Serum, qualified, heat inactivated, E.U.-approved, South America Origin	Fisher Scientific (Leicestershire, UK)	# 11550356	Cell culture
Phosphate-buffered saline (PBS)	N/A	N/A	Cell culture
ImmunoCult™-XF T-Cell Expansion Medium	Stemcell TM Technologies (Van, CA)	# 10981	Cell culture
Recombinant Human IL-2	PeproTech (LND, GB-ENG)	# 200-02	Cell culture
Recombinant Human IL-7 (10µl)	PeproTech (LND, GB-ENG)	# 200-07	Cell culture
Recombinant Human Il-15 (10µl)	PeproTech (LND, GB-ENG)	# 200-15	Cell culture
ImmunoCult™ Human CD3/CD28 T-Cell Activator	StemCell TM Technologies (Van, CA)	# 10971	Cell culture
Penicillin-Streptomycin	Thermo Fisher (MA, USA)	# 15140122	Cell culture
Alt-R® S.p. Cas9 Nuclease V3, 500 µg	INTEGRATED DNA TECHNOLOGIES (IDT) (IA, USA)	# 1081059	Electroporation
Electroporation Buffer	MaxCyte® (MD, USA)	# EPB-1	Electroporation
DNeasy Blood&Tissue gDNA extraction kit	Qiagen (DEU)	# 69581	DNA extraction
Qubit™ dsDNA HS Assay Kit	Thermo Fisher (MA, USA)	# Q32854	DNA extraction
ddPCR Supermix for Probes (No dUTP)	Bio-Rad (CA, USA)	# 1863024	ddPCR
ddPCR plates, 96 well, semi-skirted	Bio-Rad (CA, USA)	# 12001925	ddPCR
ADA2 materials (ICE primers & ddPCR reference probe)	Integrated DNA Technologies (IDT) (IA, USA)	N/A	ddPCR
Pierce™ RIPA Buffer	Thermo Fisher Scientific (MA, USA)	# 89901	BCA assay

Halt Protease Inhibitor Cocktail (100X) 1	Thermo Fisher Scientific (MA, USA)	# 78430	BCA assay
Pierce Concentrator 10K MWCO, 0.5 ml	Fisher Scientific (Leicestershire, UK)	# 88513	BCA assay
Pierce™BCA Protein Assay	Thermo Fisher Scientific (MA, USA)	# 23225	BCA assay
Adenosine deaminase (ADA) assay kit	Diazyme Laboratories, (Poway, USA)	# DZ117A	ADA2 activity test
96 well plate (black)			ADA2 activity test
erythro-9-(2-Hydroxy-3-nonyl) adenine	StemCell™ Technologies (Van, CA)	# 72442	ADA2 activity test
Saline (NaCl) 0,9%			ADA2 activity test
Total RNA Purification Kit	Norgen Biotek Corp., (CA)	# 37500	RNA extraction
RNase Away™ Decontamination Reagent	Thermo Fischer Scientific (MA, USA)	# 7002	RNA extraction
SuperScript™ VILO™ cDNA Synthesis Kit / 50 reactions	Thermo Fischer Scientific (MA, USA)	# 11754050	cDNA synthesis
SSoAdvanced Universal SYBR Green Supermix	Bio-Rad (CA, USA)	# 1725270	qPCR
qPCR primers (forward and reverse SS18)		N/A	qPCR
qPCR primers (forward and reverse ADA2)		N/A	qPCR
RNase free water	N/A	N/A	qPCR
Nano filtrated H2O	N/A	N/A	qPCR
Water, nuclease free	ThermoFisher (MA, USA)	# R0581	qPCR
Multiply®-µStrip 0,2 ml chain	Sarstedt AG & Co (DE)	# 72.985.002	qPCR
RQ1 RNase-free DNase set M6101	Promega Corporation (WI, USA)	# M6101	Flow Cytometry
Phytohemagglutinin-L (PHA-L)	Millipore Sigma (ON, Canada)	# 11249738001	Flow Cytometry
Dynabeads™ Human T-Activator CD3/CD28 for T-Cell Expansion and Activation	ThermoFisher (MA, USA)	# 11161D	Flow Cytometry
CellTrace™ CFSE Cell Proliferation Kit	ThermoFisher (MA, USA)	# C34554	Flow Cytometry
UltraComp eBeads™ Compensation Beads	Thermo Fisher (MA, USA)	# 01-2222-41	Flow Cytometry
eBioscience™ Fixable Viability Dye eFluor™ 660	ThermoFisher (MA, USA)	# 65-0864-18	Flow Cytometry

Falcon® 96-well Clear Round Bottom Not Treated Microplate	Corning Inc. (MA, USA)	# 351177	Flow Cytometry
Nunc™ 96-Well Polystyrene Conical Bottom MicroWell™ Plates	ThermoFisher (MA, USA)	# 249935	Flow Cytometry
CD3 eBioscience™	Monoclonal Antibody (OKT3), Functional Grade,	# 16-0037-81	ThermoFisher
CD28	Monoclonal Antibody (CD28.2), Functional Grade	# 16-0289-81	ThermoFisher
CFSE	CellTrace™ CFSE Proliferation Kit, for flow cytometry	# C34554	Thermo Fisher

Table 2 List of fluorescently labeled antibodies used in the flow cytometry activation assays, with the corresponding distributor, catalog number and amount used for each reaction.

Antibody/ Target	Conjugate	Selected dilution	Distributor	Product number
CD4	BV421 Mouse Anti-Human	1/100	BD Biosciences	# 562424
CD8	Brilliant Violet 570™ anti-Human	1/50	BioLegend	# 301038
CD3	APC/Fire™ 750 Anti-Mouse	1/50	BioLegend	# 300470
CD69	BV786 Mouse Anti-Human	1/80	BD Biosciences	# 563834
CD25	PE-CF594 Mouse Anti-Human	1/300	BD Biosciences	# 562525
FVD660	EBioScience™ Fixable Viability Dye eFluor™ 660	1/3000	Thermo Fisher	# 65-0864-18

Table 3 List of fluorescently labeled antibodies used in the flow cytometry proliferation assays, with the corresponding distributor, catalog number and amount used for each reaction.

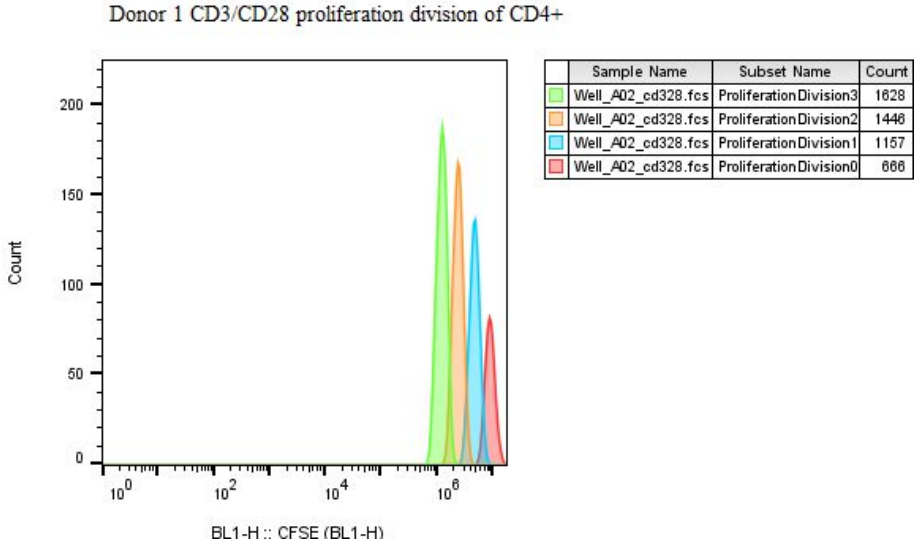
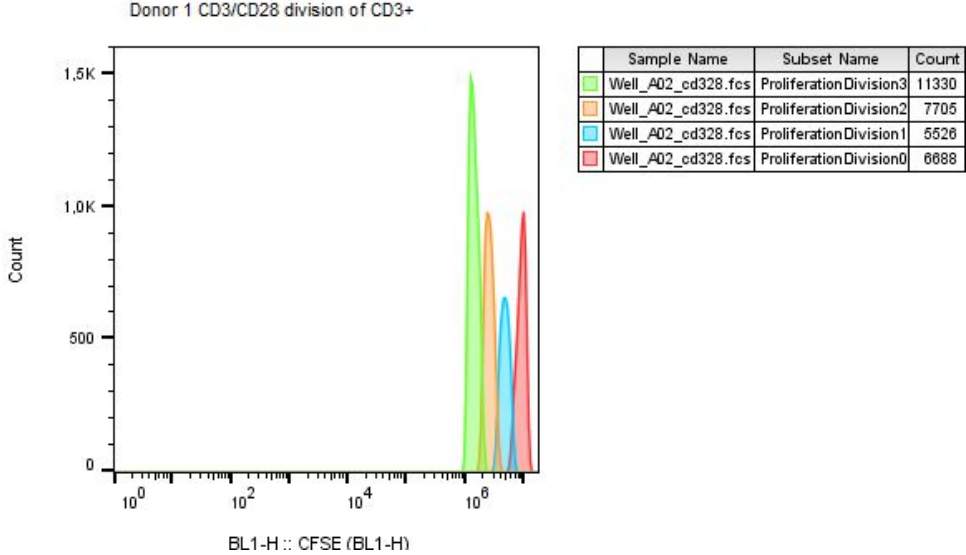
Antibody/ Target	Conjugate	Selected dilution	Distributor	Product number
CD4	BV421 Mouse Anti-Human	1/100	BD Biosciences	# 562424
CD8	PE-Cy™7	1/50	BD Biosciences	# 335822
CD3	BV605 Mouse Anti-Human	1/50	BD Biosciences	# 563219
FVD660	EBioScience™ Fixable Viability Dye eFluor™ 660	1/3000	Thermo Fisher	# 65-0864-18

Table 4 Instruments used during the project, with the corresponding distributor, catalog number and assays of usage.

Name	Distributor	Catalog number	Usage
Lonza 4D Nucleofector System, Core Unit (software 2.1)	Lonza Group AG (CH)	# AAF-1002B	Electroporation
Infinite® M Nano, single-mode microplate reader, monochromator optics	Tecan (CH)	# 30190086	ADA2 activity test, BCA assay
Qubit 4 Fluorometer	Thermo Fisher (MA, USA)	# Q33238	DNA measurement
Automated Droplet Generator	Bio-Rad (CA, USA)	# 1864101	ddPCR
QX200 Droplet Reader	Bio-Rad (CA, USA)	# 1864003	ddPCR
T100 Thermal Cycler	Bio-Rad (CA, USA)	# 1861096	ddPCR, cDNA synthesis
CFX Opus 96 Real-Time PCR system	Bio-Rad (CA, USA)	# 12011319	qPCR
NanoDrop™ 2000/2000c Spectrophotometer	Thermo Fisher (MA, USA)	# ND2000	DNA measurement
iQue® 3 Advanced Flow Cytometry System	Sartorius (AG, DE)	# 91377	Flow Cytometry

6 Appendix II

Proliferation index of cd3 cd4 and cd8 of short cultivated T-cells:



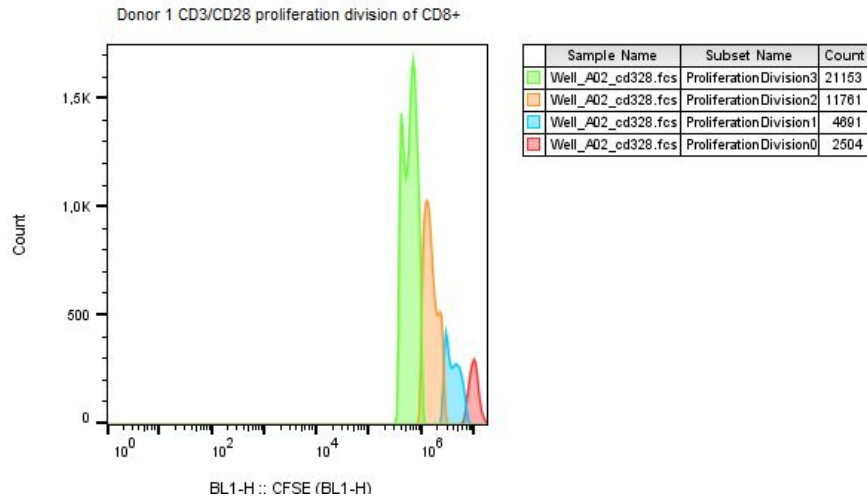
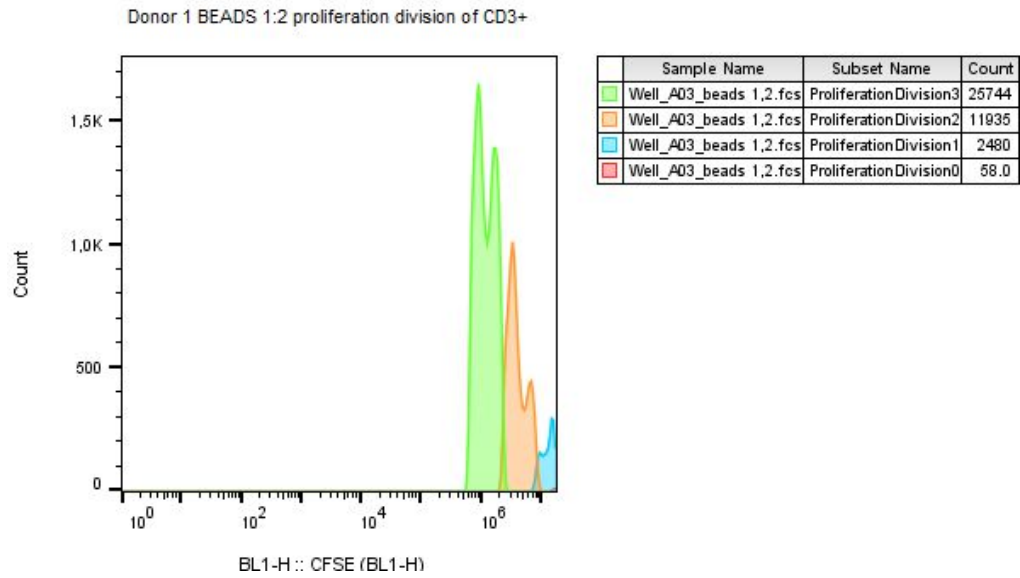
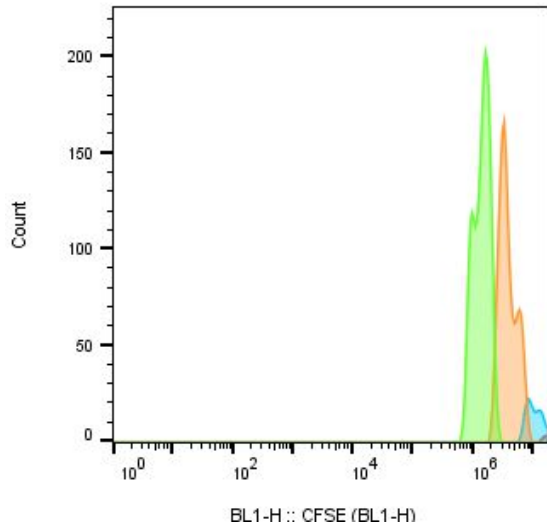


Figure A1-A3: donor 1 stimulated with CD3/CD28, divisions of CD3+, CD4+ and CD8+.

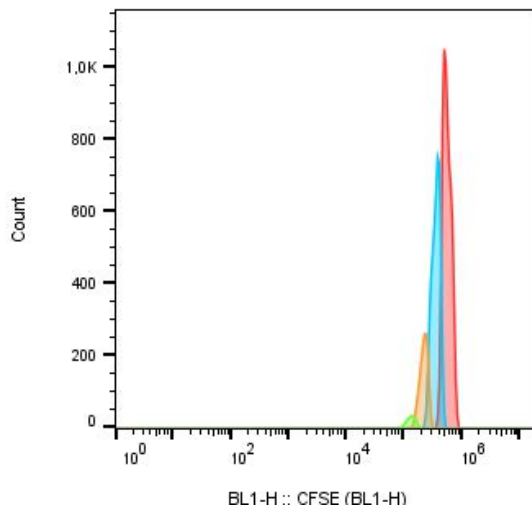


Donor 1 BEADS 1:2 proliferation division of CD4+



Sample Name	Subset Name	Count
Well_A03_beads 1,2.fcs	ProliferationDivision3	2475
Well_A03_beads 1,2.fcs	ProliferationDivision2	1889
Well_A03_beads 1,2.fcs	ProliferationDivision1	274
Well_A03_beads 1,2.fcs	ProliferationDivision0	22.0

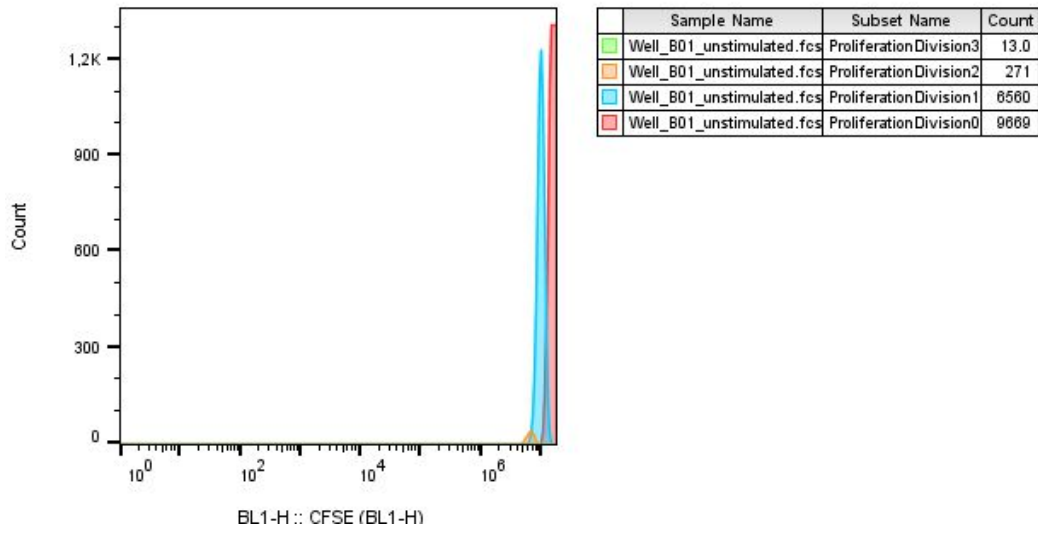
Donor 1 BEADS 1:2 proliferation division of CD8+



Sample Name	Subset Name	Count
Well_A03_beads 1,2.fcs	ProliferationDivision3	297
Well_A03_beads 1,2.fcs	ProliferationDivision2	1747
Well_A03_beads 1,2.fcs	ProliferationDivision1	5129
Well_A03_beads 1,2.fcs	ProliferationDivision0	7174

Figure A4-A6: donor 1 stimulated with CD3/CD28 BEADS, divisions of CD3+, CD4+ and CD8+.

Donor 2 unstimulated proliferation division of CD3+



Donor 2 unstimulated proliferation division of CD8+

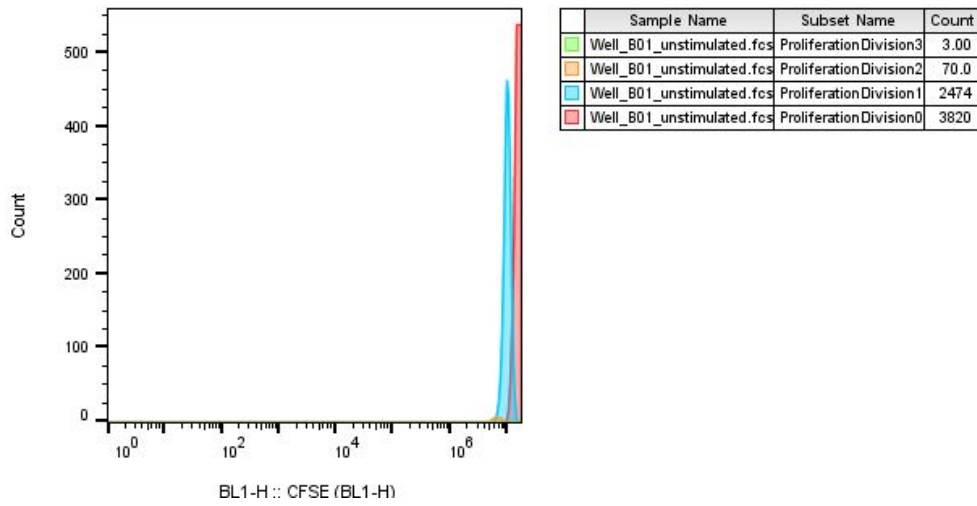
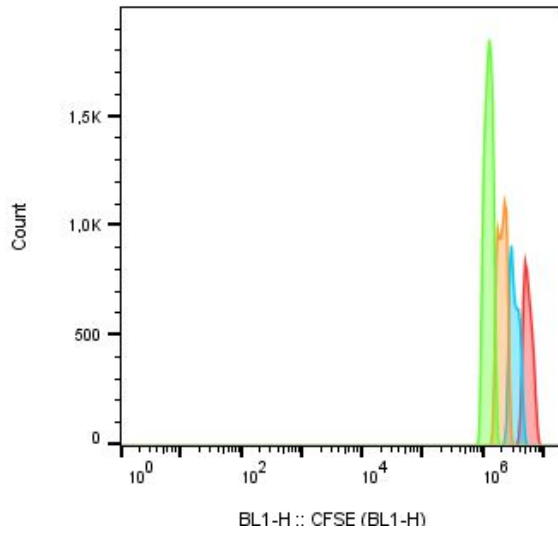


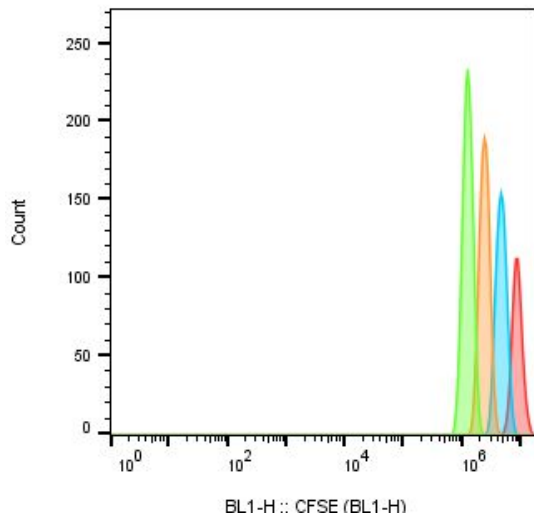
Figure A7-A8: donor 2 unstimulated, divisions of CD3+ and CD8+.

Donor 2 CD3/CD28 proliferation division of CD3+



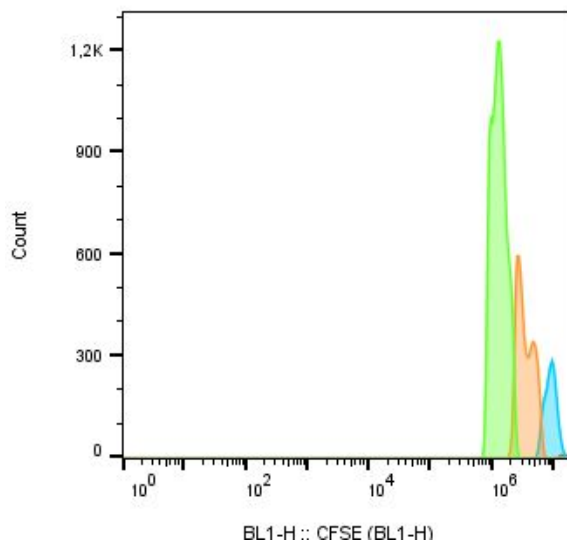
	Sample Name	Subset Name	Count
■	Well_B02_cd328.fcs	ProliferationDivision3	13139
■	Well_B02_cd328.fcs	ProliferationDivision2	8777
■	Well_B02_cd328.fcs	ProliferationDivision1	8329
■	Well_B02_cd328.fcs	ProliferationDivision0	5711

Donor 2 CD3/CD28 proliferation division of CD4+



	Sample Name	Subset Name	Count
■	Well_B02_cd328.fcs	ProliferationDivision3	1880
■	Well_B02_cd328.fcs	ProliferationDivision2	1581
■	Well_B02_cd328.fcs	ProliferationDivision1	1342
■	Well_B02_cd328.fcs	ProliferationDivision0	878

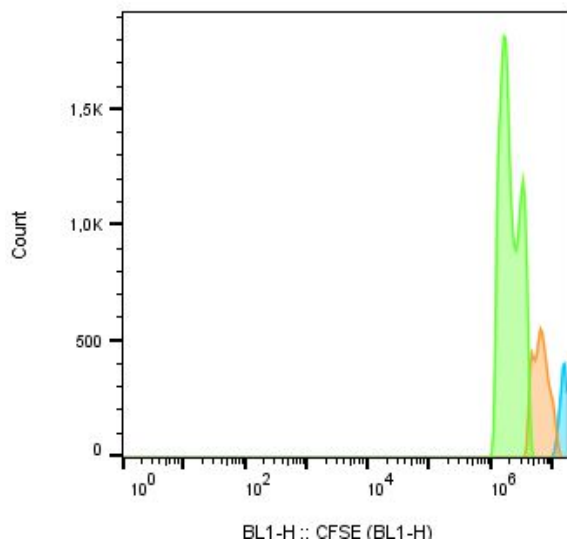
Donor 2 CD3/CD28 proliferation division of CD8+



	Sample Name	Subset Name	Count
■	Well_B02_cd328.fcs	ProliferationDivision3	14822
■	Well_B02_cd328.fcs	ProliferationDivision2	6478
■	Well_B02_cd328.fcs	ProliferationDivision1	2569
■	Well_B02_cd328.fcs	ProliferationDivision0	95.0

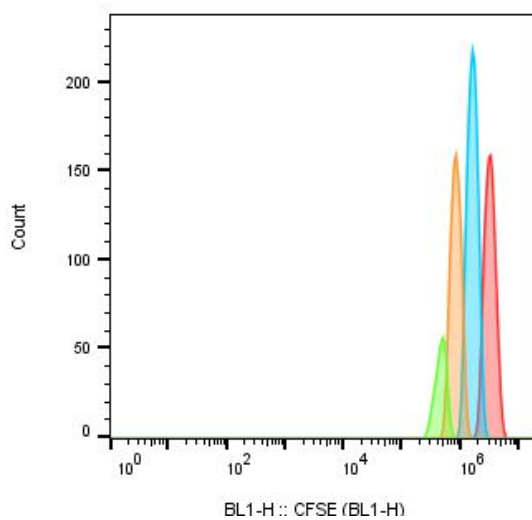
Figure A9-A11: donor 2 stimulated with CD3/CD28, divisions of CD3+, CD4+ and CD8+.

Donor 2 BEADS 1:2 proliferation division of CD3+



Sample Name	Subset Name	Count
Well_B03_beads 1,2.fcs	ProliferationDivision3	24993
Well_B03_beads 1,2.fcs	ProliferationDivision2	6859
Well_B03_beads 1,2.fcs	ProliferationDivision1	2138
Well_B03_beads 1,2.fcs	ProliferationDivision0	0

Donor 2 BEADS 1:2 proliferation division of CD4+



Sample Name	Subset Name	Count
Well_B03_beads 1,2.fcs	ProliferationDivision3	502
Well_B03_beads 1,2.fcs	ProliferationDivision2	1427
Well_B03_beads 1,2.fcs	ProliferationDivision1	1958
Well_B03_beads 1,2.fcs	ProliferationDivision0	1470

Donor 2 BEADS 1:2 proliferation division of CD8+

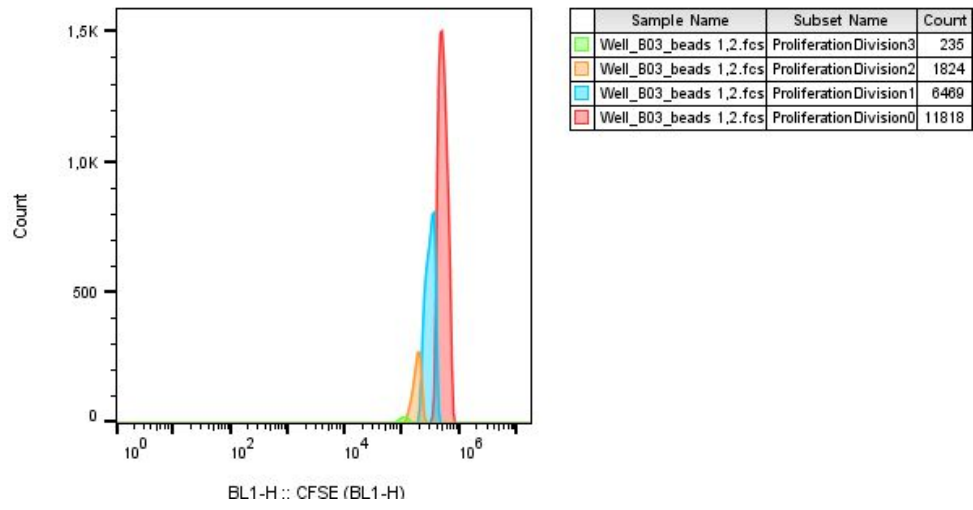


Figure A12-A14: donor 2 stimulated with CD3/CD28 BEADS, divisions of CD3+, CD4+ and CD8+.

7 References

- 3 - CLUSTER OF DIFFERENTIATION (CD) ANTIGENS. (2004). In J. M. Cruse, R. E. Lewis, & H. Wang (Eds.), *Immunology Guidebook* (pp. 47-124). Academic Press. <https://doi.org/https://doi.org/10.1016/B978-012198382-6/50027-3>
- Abdelnour, S. A., Xie, L., Hassanin, A. A., Zuo, E., & Lu, Y. (2021). The Potential of CRISPR/Cas9 Gene Editing as a Treatment Strategy for Inherited Diseases [Review]. *Frontiers in Cell and Developmental Biology*, 9. <https://doi.org/10.3389/fcell.2021.699597>
- Adli, M. (2018). The CRISPR tool kit for genome editing and beyond. *Nature Communications*, 9(1), 1911. <https://doi.org/10.1038/s41467-018-04252-2>
- Akadeum Life Sciences. (2020). *What are Naïve Cells? Naïve T Cell, Naïve B Cell, and How to Isolate Naïve Lymphocytes*. Retrieved 27.04.2023 from
- Aksentijevich I, Sampaio Moura N, & K., B. (2019). Adenosine Deaminase 2 Deficiency. *GeneReviews® [Internet], Seattle (WA): University of Washington, Seattle; 1993-2022*. <https://doi.org/https://www.ncbi.nlm.nih.gov/books/NBK544951/>
- Al-Herz, W., Bousfiha, A., Casanova, J. L., Chatila, T., Conley, M. E., Cunningham-Rundles, C., Etzioni, A., Franco, J. L., Gaspar, H. B., Holland, S. M., Klein, C., Nonoyama, S., Ochs, H. D., Oksenhendler, E., Picard, C., Puck, J. M., Sullivan, K., & Tang, M. L. (2014). Primary immunodeficiency diseases: an update on the classification from the international union of immunological societies expert committee for primary immunodeficiency. *Front Immunol*, 5, 162. <https://doi.org/10.3389/fimmu.2014.00162>
- Aristizábal, B., & González, Á. (2013). Innate immune system. In J. Anaya, Y. Shoenfeld, A. Rojas-Villarraga, R. A. Levy, & R. Cervera (Eds.), *Autoimmunity From Bench to Bedside* (1 ed., pp. 1-2). El Rosario University Press.
- B. Alberts, A. Johnson, J. Lewis, & al., e. (2002a). Helper T Cells and Lymphocyte Activation. In *Molecular Biology of the Cell* (4 ed.). Garland Science.
- B. Alberts, A. Johnson, J. Lewis, & al., e. (2002b). T Cells and MHC Proteins. In *Molecular Biology of the Cell* (4 ed.). Garland Science.
- Bajnok, A., Ivanova, M., Rigó, J., & Toldi, G. (2017). The Distribution of Activation Markers and Selectins on Peripheral T Lymphocytes in Preeclampsia. *Mediators of Inflammation*, 2017, 1-7. <https://doi.org/10.1155/2017/8045161>
- Banchereau, J., Briere, F., Caux, C., Davoust, J., Lebecque, S., Liu, Y.-J., Pulendran, B., & Palucka, K. (2000). Immunobiology of Dendritic Cells. *Annual Review of Immunology*, 18(1), 767-811. <https://doi.org/10.1146/annurev.immunol.18.1.767>
- Ben-Ami, T., Revel-Vilk, S., Brooks, R., Shaag, A., Hershfield, M. S., Kelly, S. J., Ganson, N. J., Kfir-Erenfeld, S., Weintraub, M., Elpeleg, O., Berkun, Y., & Stepensky, P. (2016). Extending the Clinical Phenotype of Adenosine Deaminase 2 Deficiency. *J Pediatr*, 177, 316-320. <https://doi.org/10.1016/j.jpeds.2016.06.058>
- Bio-Rad. Digital Droplet PCR Applications Guide.
- Bio-Rad. QX200 Droplet Reader and Qantasoft Software.
- Borges, O., Borchard, G., de Sousa, A., Junginger, H. E., & Cordeiro-da-Silva, A. (2007). Induction of lymphocytes activated marker CD69 following exposure to chitosan and alginate biopolymers. *International Journal of Pharmaceutics*, 337(1), 254-264. <https://doi.org/https://doi.org/10.1016/j.ijpharm.2007.01.021>
- Boston Children's Hospital. (2017). Patients' individual genomes may affect efficacy, safety of gene editing: CRISPR-Cas9 and other gene editing systems may need to be customized to the patient. *ScienceDaily*.

- Bowers, S. M., Gibson, K. M., Cabral, D. A., & Brown, K. L. (2020). Adenosine deaminase 2 activity negatively correlates with age during childhood. *Pediatr Rheumatol Online J*, 18(1), 54. <https://doi.org/10.1186/s12969-020-00446-5>
- Brodin, P., & Davis, M. M. (2017). Human immune system variation. *Nat Rev Immunol*, 17(1), 21-29. <https://doi.org/10.1038/nri.2016.125>
- Chakrabarti, A. M., Henser-Brownhill, T., Monserrat, J., Poetsch, A. R., Luscombe, N. M., & Scaffidi, P. (2019). Target-Specific Precision of CRISPR-Mediated Genome Editing. *Molecular Cell*, 73(4), 699-713.e696. <https://doi.org/10.1016/j.molcel.2018.11.031>
- Chattopadhyay, P. K., & Roederer, M. (2010). Good cell, bad cell: flow cytometry reveals T-cell subsets important in HIV disease. *Cytometry A*, 77(7), 614-622. <https://doi.org/10.1002/cyto.a.20905>
- Chen, C. L., Rodiger, J., Chung, V., Viswanatha, R., Mohr, S. E., Hu, Y., & Perrimon, N. (2020). SNP-CRISPR: A Web Tool for SNP-Specific Genome Editing. *G3 (Bethesda)*, 10(2), 489-494. <https://doi.org/10.1534/g3.119.400904>
- Cibrián, D., & Sánchez-Madrid, F. (2017). CD69: from activation marker to metabolic gatekeeper. *European Journal of Immunology*, 47(6), 946-953. <https://doi.org/10.1002/eji.201646837>
- Collino, C. J. G., Jaldin-Finca, J. R., & Chiabrando, G. A. (2007). Statistical criteria to establish optimal antibody dilution in flow cytometry analysis. *Cytometry Part B: Clinical Cytometry*, 72B(3), 223-226. <https://doi.org/10.1002/cyto.b.20158>
- Cox, D. L., & Nelson, M. (2021). *Lehninger Principles of Biochemistry* (8th ed.). W.H. Freeman & Company.
- Delfs, M. W., Furukawa, Y., Mitchell, R. N., & Lichtman, A. H. (2001). CD8+ T CELL SUBSETS TC1 AND TC2 CAUSE DIFFERENT HISTOPATHOLOGIC FORMS OF MURINE CARDIAC ALLOGRAFT REJECTION1. *Transplantation*, 71(5), 606-610. https://journals.lww.com/transplantjournal/Fulltext/2001/03150/CD8_T_CELL_SUBSETS_TC1_AND_TC2_CAUSE_DIFFERENT.5.aspx
- Dolezal, T., Dolezelova, E., Zurovec, M., & Bryant, P. J. (2005). A role for adenosine deaminase in Drosophila larval development. *PLoS Biol*, 3(7), e201. <https://doi.org/10.1371/journal.pbio.0030201>
- Doudna, J. A. (2020). The promise and challenge of therapeutic genome editing. *Nature*, 578(7794), 229-236. <https://doi.org/10.1038/s41586-020-1978-5>
- Dropulic, L. K., & Lederman, H. M. (2016). Overview of Infections in the Immunocompromised Host. *Microbiol Spectr*, 4(4). <https://doi.org/10.1128/microbiolspec.DMIH2-0026-2016>
- Esensten, J. H., Helou, Y. A., Chopra, G., Weiss, A., & Bluestone, J. A. (2016). CD28 Costimulation: From Mechanism to Therapy. *Immunity*, 44(5), 973-988. <https://doi.org/10.1016/j.immuni.2016.04.020>
- Flinn, A. M., & Gennery, A. R. (2018). Adenosine deaminase deficiency: a review. *Orphanet Journal of Rare Diseases*, 13(1), 65. <https://doi.org/10.1186/s13023-018-0807-5>
- Hashem, H., Egler, R., & Dalal, J. (2017). Refractory Pure Red Cell Aplasia Manifesting as Deficiency of Adenosine Deaminase 2. *Journal of Pediatric Hematology/Oncology*, 39(5), e293-e296. <https://doi.org/10.1097/mpH.0000000000000805>
- He, X., Tan, C., Wang, F., Wang, Y., Zhou, R., Cui, D., You, W., Zhao, H., Ren, J., & Feng, B. (2016). Knock-in of large reporter genes in human cells via CRISPR/Cas9-induced homology-dependent and independent DNA repair. *Nucleic Acids Research*, 44(9), e85-e85. <https://doi.org/10.1093/nar/gkw064>

- Hoggatt, J., & Pelus, L. M. (2013). Hematopoiesis. In S. Maloy & K. Hughes (Eds.), *Brenner's Encyclopedia of Genetics (Second Edition)* (pp. 418-421). Academic Press. <https://doi.org/10.1016/B978-0-12-374984-0.00686-0>
- Iwasaki, A., & Medzhitov, R. (2010). Regulation of Adaptive Immunity by the Innate Immune System. *Science*, 327(5963), 291-295. <https://doi.org/10.1126/science.1183021>
- Jagannathan-Bogdan, M., & Zon, L. I. (2013). Hematopoiesis. *Development*, 140(12), 2463-2467. <https://doi.org/10.1242/dev.083147>
- Janeway, C. A., & Bottomly, K. (1994). Signals and signs for lymphocyte responses. *Cell*, 76(2), 275-285. [https://doi.org/10.1016/0092-8674\(94\)90335-2](https://doi.org/10.1016/0092-8674(94)90335-2)
- Janeway CA Jr, Travers P, Walport M, & al., e. (2001). General properties of armed effector T cells. In *Immunobiology: The Immune System in Health and Disease* (5th edition ed.). Garland Science.
- Jee, H., Huang, Z., Baxter, S., Huang, Y., Taylor, M. L., Henderson, L. A., Rosenzweig, S., Sharma, A., Chambers, E. P., Hershfield, M. S., Zhou, Q., Dedeoglu, F., Aksentijevich, I., Nigrovic, P. A., O'Donnell-Luria, A., & Lee, P. Y. (2022). Comprehensive analysis of ADA2 genetic variants and estimation of carrier frequency driven by a function-based approach. *Journal of Allergy and Clinical Immunology*, 149(1), 379-387. <https://doi.org/10.1016/j.jaci.2021.04.034>
- Jinek, M., Chylinski, K., Fonfara, I., Hauer, M., Doudna, J. A., & Charpentier, E. (2012). A programmable dual-RNA-guided DNA endonuclease in adaptive bacterial immunity. *Science*, 337(6096), 816-821. <https://doi.org/10.1126/science.1225829>
- Kaljas, Y., Liu, C., Skaldin, M., Wu, C., Zhou, Q., Lu, Y., Aksentijevich, I., & Zavialov, A. V. (2017). Human adenosine deaminases ADA1 and ADA2 bind to different subsets of immune cells. *Cellular and Molecular Life Sciences*, 74(3), 555-570. <https://doi.org/10.1007/s00018-016-2357-0>
- Kleiveland, C. R. (2015). Peripheral blood mononuclear cells. *The Impact of Food Bioactives on Health: in vitro and ex vivo models*, 161-167.
- Kondo, M. (2010). Lymphoid and myeloid lineage commitment in multipotent hematopoietic progenitors. *Immunol Rev*, 238(1), 37-46. <https://doi.org/10.1111/j.1600-065X.2010.00963.x>
- Lino, C. A., Harper, J. C., Carney, J. P., & Timlin, J. A. (2018). Delivering CRISPR: a review of the challenges and approaches. *Drug Deliv*, 25(1), 1234-1257. <https://doi.org/10.1080/10717544.2018.1474964>
- Luckheeram, R. V., Zhou, R., Verma, A. D., & Xia, B. (2012). CD4⁺T cells: differentiation and functions. *Clin Dev Immunol*, 2012, 925135. <https://doi.org/10.1155/2012/925135>
- Luckheeram, R. V., Zhou, R., Verma, A. D., & Xia, B. (2012). CD4⁺T Cells: Differentiation and Functions. *Clinical and Developmental Immunology*, 2012, 925135. <https://doi.org/10.1155/2012/925135>
- MacPherson, S., Keyes, S., Kilgour, M. K., Smazynski, J., Chan, V., Sudderth, J., Turcotte, T., Devlieger, A., Yu, J., Huggler, K. S., Cantor, J. R., DeBerardinis, R. J., Siatskas, C., & Lum, J. J. (2022). Clinically relevant T cell expansion media activate distinct metabolic programs uncoupled from cellular function. *Molecular Therapy - Methods & Clinical Development*, 24, 380-393. <https://doi.org/10.1016/j.omtm.2022.02.004>
- McKinnon, K. M. (2018). Flow Cytometry: An Overview. *Curr Protoc Immunol*, 120, 5.1.1-5.1.11. <https://doi.org/10.1002/cpim.40>
- Meyts, I., & Aksentijevich, I. (2018). Deficiency of Adenosine Deaminase 2 (DADA2): Updates on the Phenotype, Genetics, Pathogenesis, and Treatment. *J Clin Immunol*, 38(5), 569-578. <https://doi.org/10.1007/s10875-018-0525-8>

- Meyts, I., & Aksentijevich, I. (2018). Deficiency of Adenosine Deaminase 2 (DADA2): Updates on the Phenotype, Genetics, Pathogenesis, and Treatment. *Journal of Clinical Immunology*, 38(5), 569-578. <https://doi.org/10.1007/s10875-018-0525-8>
- Moens, L., Hershfield, M., Arts, K., Aksentijevich, I., & Meyts, I. (2019). Human adenosine deaminase 2 deficiency: A multi-faceted inborn error of immunity. *Immunological Reviews*, 287(1), 62-72. <https://doi.org/10.1111/imr.12722>
- Ortolani, C. (2022). *Flow Cytometry Today - Everything You Need to Know about Flow Cytometry* (1 ed.). Springer Cham. <https://doi.org/10.1007/978-3-031-10836-5>
- Parham, P. (2021). *the immune system* (B. Twitchell, Ed. fifth ed.). W.W. Norton & Company. Inc.
- Pennock, N. D., White, J. T., Cross, E. W., Cheney, E. E., Tamburini, B. A., & Kedl, R. M. (2013). T cell responses: naive to memory and everything in between. *Adv Physiol Educ*, 37(4), 273-283. <https://doi.org/10.1152/advan.00066.2013>
- Quah, B. J., & Parish, C. R. (2010). The use of carboxyfluorescein diacetate succinimidyl ester (CFSE) to monitor lymphocyte proliferation. *J Vis Exp*(44). <https://doi.org/10.3791/2259>
- Ramstead, A. G., & Jutila, M. A. (2012). Complex role of $\gamma\delta$ T-cell-derived cytokines and growth factors in cancer. *J Interferon Cytokine Res*, 32(12), 563-569. <https://doi.org/10.1089/jir.2012.0073>
- Raza, Y., Salman, H., & Luberto, C. (2021). Sphingolipids in Hematopoiesis: Exploring Their Role in Lineage Commitment. *Cells*, 10(10), 2507. <https://www.mdpi.com/2073-4409/10/10/2507>
- Reddy, M., Eirikis, E., Davis, C., Davis, H. M., & Prabhakar, U. (2004). Comparative analysis of lymphocyte activation marker expression and cytokine secretion profile in stimulated human peripheral blood mononuclear cell cultures: an in vitro model to monitor cellular immune function. *Journal of Immunological Methods*, 293(1), 127-142. <https://doi.org/10.1016/j.jim.2004.07.006>
- Sánchez-Ramón, S., Bermúdez, A., González-Granado, L. I., Rodríguez-Gallego, C., Sastre, A., & Soler-Palacín, P. (2019). Primary and Secondary Immunodeficiency Diseases in Oncohaematology: Warning Signs, Diagnosis, and Management. *Front Immunol*, 10, 586. <https://doi.org/10.3389/fimmu.2019.00586>
- Shah, K., Al-Haidari, A., Sun, J., & Kazi, J. U. (2021). T cell receptor (TCR) signaling in health and disease. *Signal Transduction and Targeted Therapy*, 6(1), 412. <https://doi.org/10.1038/s41392-021-00823-w>
- Starr, T. K., Jameson, S. C., & Hogquist, K. A. (2003). Positive and Negative Selection of T Cells. *Annual Review of Immunology*, 21(1), 139-176. <https://doi.org/10.1146/annurev.immunol.21.120601.141107>
- Stockwin, L. H., McGonagle, D., Martin, I. G., & Blair, G. E. (2000). Dendritic cells: Immunological sentinels with a central role in health and disease. *Immunology and Cell Biology*, 78(2), 91-102. <https://doi.org/10.1046/j.1440-1711.2000.00888.x>
- Sutton, D. W., Chen, P. C., & Schmid-Schönbein, G. W. (1988). Cell separation in the buffy coat. *Biorheology*, 25(4), 663-673. <https://doi.org/10.3233/bir-1988-25406>
- Taylor, S. C., Laperriere, G., & Germain, H. (2017). Droplet Digital PCR versus qPCR for gene expression analysis with low abundant targets: from variable nonsense to publication quality data. *Scientific Reports*, 7(1), 2409. <https://doi.org/10.1038/s41598-017-02217-x>
- Theoharides, T. C., Alysandratos, K.-D., Angelidou, A., Delivanis, D.-A., Sismanopoulos, N., Zhang, B., Asadi, S., Vasiadi, M., Weng, Z., Miniati, A., & Kalogeromitros, D. (2012).

- Mast cells and inflammation. *Biochimica et Biophysica Acta (BBA) - Molecular Basis of Disease*, 1822(1), 21-33. <https://doi.org/https://doi.org/10.1016/j.bbadis.2010.12.014>
- Tung, J. W., Heydari, K., Tirouvanziam, R., Sahaf, B., Parks, D. R., Herzenberg, L. A., & Herzenberg, L. A. (2007). Modern Flow Cytometry: A Practical Approach. *Clinics in Laboratory Medicine*, 27(3), 453-468. <https://doi.org/https://doi.org/10.1016/j.cll.2007.05.001>
- Van Montfrans, J. M., Hartman, E. A. R., Braun, K. P. J., Hennekam, E. A. M., Hak, E. A., Nederkoorn, P. J., Westendorp, W. F., Bredius, R. G. M., Kollen, W. J. W., Schölvinck, E. H., Legger, G. E., Meyts, I., Liston, A., Lichtenbelt, K. D., Giltay, J. C., Van Haften, G., De Vries Simons, G. M., Leavis, H., Sanders, C. J. G., . . . Van Gijn, M. E. (2016). Phenotypic variability in patients with ADA2 deficiency due to identical homozygous R169Q mutations. *Rheumatology*, 55(5), 902-910. <https://doi.org/10.1093/rheumatology/kev439>
- Vinchi, F. (2021). Towards a Cure for Adenosine Deaminase 2 Deficiency Through Genetic Correction of Macrophage Polarization. *Hemasphere*, 5(11), e653. <https://doi.org/10.1097/hs9.0000000000000653>
- Vivier, E., Raullet, D. H., Moretta, A., Caligiuri, M. A., Zitvogel, L., Lanier, L. L., Yokoyama, W. M., & Ugolini, S. (2011). Innate or Adaptive Immunity? The Example of Natural Killer Cells. *Science*, 331(6013), 44-49. <https://doi.org/doi:10.1126/science.1198687>
- Vogan, K. (2014). Inflammatory syndrome ADA2 deficiency. *Nature Genetics*, 46(4), 325-325. <https://doi.org/10.1038/ng.2943>
- Yang, H., Parkhouse, R. M., & Wileman, T. (2005). Monoclonal antibodies that identify the CD3 molecules expressed specifically at the surface of porcine gammadelta-T cells. *Immunology*, 115(2), 189-196. <https://doi.org/10.1111/j.1365-2567.2005.02137.x>
- Yarmush, M. L., Golberg, A., Serša, G., Kotnik, T., & Miklavčič, D. (2014). Electroporation-Based Technologies for Medicine: Principles, Applications, and Challenges. *Annual Review of Biomedical Engineering*, 16(1), 295-320. <https://doi.org/10.1146/annurev-bioeng-071813-104622>
- Zavialov, Andrey V., & Engström, Å. (2005). Human ADA2 belongs to a new family of growth factors with adenosine deaminase activity. *Biochemical Journal*, 391(1), 51-57. <https://doi.org/10.1042/bj20050683>
- Zavialov, A. V., Gracia, E., Glaichenhaus, N., Franco, R., Zavialov, A. V., & Lauvau, G. (2010). Human adenosine deaminase 2 induces differentiation of monocytes into macrophages and stimulates proliferation of T helper cells and macrophages. *Journal of Leukocyte Biology*, 88(2), 279-290. <https://doi.org/10.1189/jlb.1109764>
- Zavialov, A. V., Yu, X., Spillmann, D., Lauvau, G., & Zavialov, A. V. (2010). Structural Basis for the Growth Factor Activity of Human Adenosine Deaminase ADA2*♦. *Journal of Biological Chemistry*, 285(16), 12367-12377. <https://doi.org/https://doi.org/10.1074/jbc.M109.083527>
- Zhang, B. (2021). CRISPR/Cas gene therapy. *Journal of Cellular Physiology*, 236(4), 2459-2481. <https://doi.org/https://doi.org/10.1002/jcp.30064>
- Zhu, J., & Paul, W. E. (2008). CD4 T cells: fates, functions, and faults. *Blood*, 112(5), 1557-1569. <https://doi.org/10.1182/blood-2008-05-078154>



Norges miljø- og biovitenskapelige universitet
Noregs miljø- og biovitenskapelige universitet
Norwegian University of Life Sciences

Postboks 5003
NO-1432 Ås
Norway